

Test of 1st YBCO Helical Solenoid Double Pancake Model

M. Yu, E. Barzi, V. Lombardo, M.L. Lopes, D. Turrioni, A.V. Zlobin
Fermilab, Technical Division;

G. Flanagan, Muons Inc.

1. Introduction

A helical cooling channel (HCC) has been proposed for six-dimension (6D) cooling of muon beams [1]. It is based on a continuous absorber and RF cavities imbedded into superconducting magnets which superimpose solenoid, helical dipole and helical gradient field components. The HCC for muon collider is divided into several sections, each section with progressively stronger fields, smaller aperture and shorter helix to achieve the optimal muon cooling rate [2].

For the HCC low-field section, a four-coil helical solenoid (HS) with NbTi cable was designed, fabricated [3] and tested [4] at Fermilab. For the HCC high-field section, due to the high magnetic field, it is suggested to investigate High Temperature Superconductors (HTS) as the coil structure [5]. Furthermore, the RF cavities inside the coil are required to operate at the temperatures above 30 K (assuming gaseous H₂ is used as the absorber), and there will be very little space to fit the thermal insulation and support structure in between the RF system and the magnets. The use of HTS can solve this problem by allowing the operation of both the magnets and RF system at the same temperature.

Therefore, development of the design and fabrication technology of a high-field HS based on HTS material is critical for realizing a practical HCC. This note describes the design, fabricating, and testing of a YBCO based HS segment. The note will discuss the first and second iterations of the HS model. The first model showed significant degradation when tested. The cause of the degradation was determined and steps were taken to address the cause. A second HS model was fabricated using the tape previously used in the first model, and the second model benefited from the fabrication improvements and did not show any significant degradation. The test results are shown and discussed in the remainder of the paper.

2. Design and Fabrication Overview

2.1. Conductor selection

Fig. 1 shows the dependences of engineering current density J_E vs. transverse magnetic field B at 4.2 K [6] for two practical HTS conductors: BSCCO-2212 round wire and YBCO tape. Since YBCO tape has a strong anisotropy with respect to the field orientation, the YBCO data are presented for both parallel (//) and perpendicular (\perp) field orientations. The helical solenoid has quite strong transverse field components, it is expected that the J_E - B dependence in the perpendicular field will determine the superconductor performance limit of the coil. In this sense, BSCCO wire and YBCO tape have comparable properties.

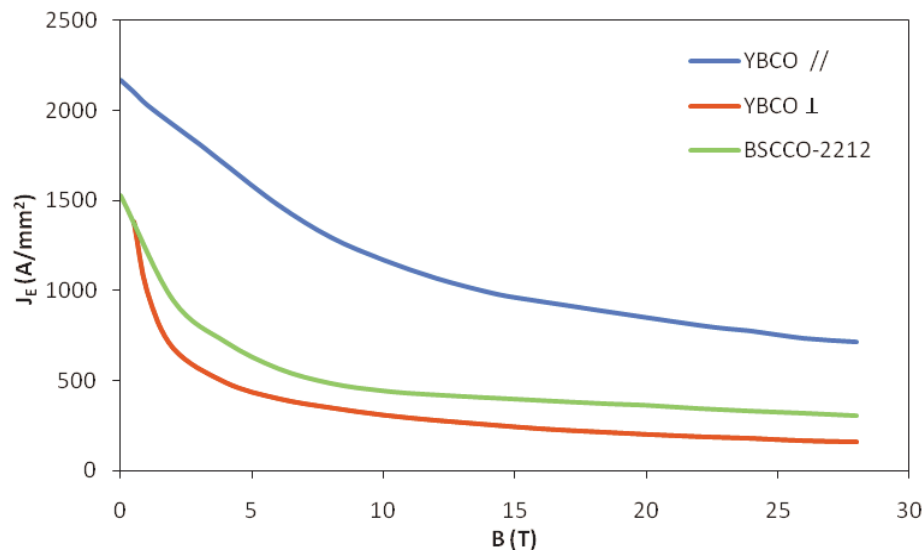


Fig. 1. J_E vs. B for BSCCO wire and YBCO tape.

BSCCO-2212 wire before the final heat treatment can be formed into multistrand round or flat cables [7] which then need to be reacted in Oxygen following a very strict heat treatment cycle. The peak temperature $\sim 890^\circ\text{C}$ needs to be well controlled (within 0.5°C for ~ 12 minutes) [8]. This process is presently hard to achieve making it difficult to guarantee I_c magnitude and homogeneity, especially for a large volume of superconductor. Additionally, BSCCO wires are very sensitive to the longitudinal and transverse strain and stress; this imposes additional requirements for the conductor support structures [9].

In contrast to BSCCO, YBCO tapes do not require the final reaction, are flexible in the easy-bend direction, and show very promising mechanical capabilities [10]. Also, YBCO presently offers better I_c performance at $T > 30$ K with respect to BSCCO-2212 wires [11]. The problem of making multi-strand cable based on YBCO tapes can be solved using the ROEBEL cable design [12]. Taking into account the aforementioned considerations, YBCO tape was selected as the baseline conductor for the HCC high-field section model.

2.2. Model Parameters

Fig. 2 shows the assembled mechanical structure of the double-pancake unit with dimensions [13]. The design of double-pancake units allows assembling all the units into a longer helical solenoid by replacing one side flange with a connecting flange that accommodates the splices between units. Moreover, the modular structure of HS allows for the inclusion of a gap between two units, the gap can be used to insert an RF cavity and feed through [14]. Both assembly configurations are shown in Fig. 3.

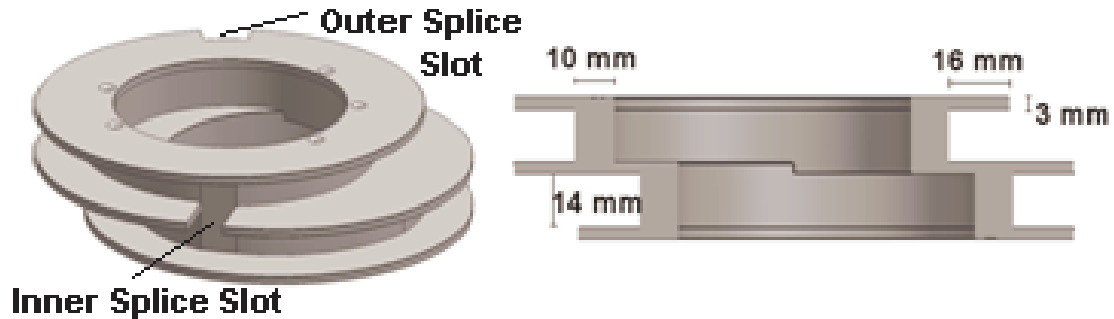


Fig. 2. A double-pancake unit support structure

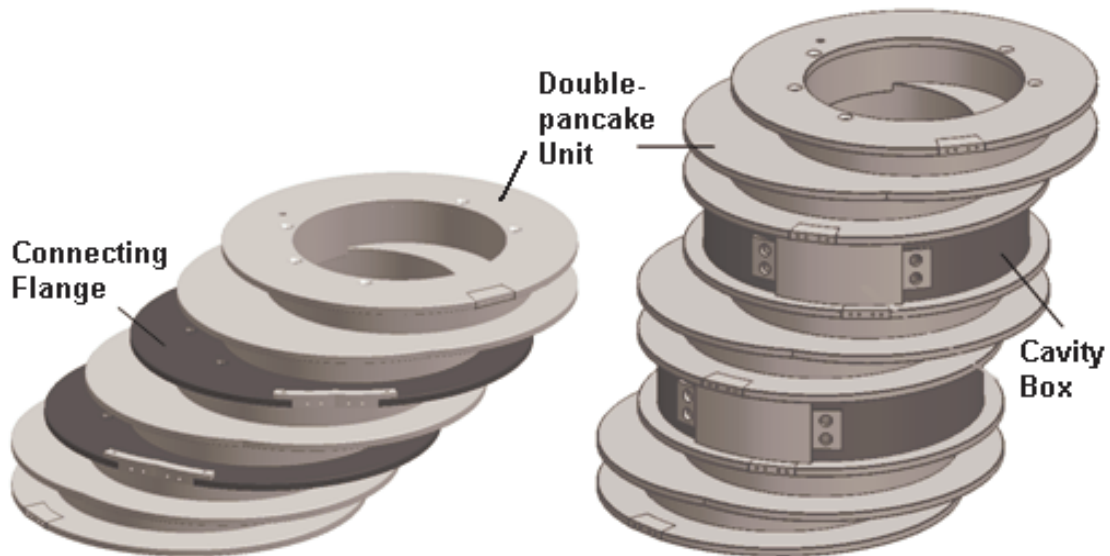


Figure 3. Assembly of three double-pancake units (left). Assembly of three double-pancake units and two cavity boxes (right).

The design parameters for the high field section of HCC are shown in Table 1. To reach the required field components, the HS, without the cavity gap in between two double-pancake units, should consist of at least 24 double-pancake units, making 2 periods of helical solenoid. The scenario that includes the embedding of RF cavities into the HS is still under conceptual design.

TABLE 1 TARGET PARAMETERS FOR HCC HIGH FIELD SECTION

Parameter	Unit	Value
Helix period	m	0.40
Orbit radius	m	0.064
Solenoidal field, B_z	T	-17.3
Helical dipole, B_t	T	4.06
Helical gradient, dB_t/dr	T/m	-4.5
Maximum field in the coil	T	21.0
Coil ID	m	0.10
Coil OD	m	0.50
Coil length	m	0.017
Number of coil per period		24

TABLE 2 HS SHORT MODELS PARAMETERS

Parameter	Unit	Number of Double-pancake Units		
		1	2	3
Coil ID	m	0.10	0.10	0.10
Coil OD	m	0.116	0.116	0.116
Number of turns/coil		58	58	58
Predicted I_{quench}	kA	1.424	1.362	1.348
Maximum Coil // Field	T	4.35	4.73	5.06
Maximum Coil \perp Field	T	3.4	3.63	3.68
Inductance	mH	1.6	4.32	7.4
Stored energy	kJ	1.62	4	6.74

The short models comprised of 1 to 3 double-pancake units were designed and the fabrication was planned. The conductor used for the coil was SCS12050 Superpower YBCO tape with a nominal $I_c(0T,77K) = 330$ A. Table 2 shows the short models parameters. From Figure 1 it can be seen that the field component perpendicular to the tape will dominate the quench current.

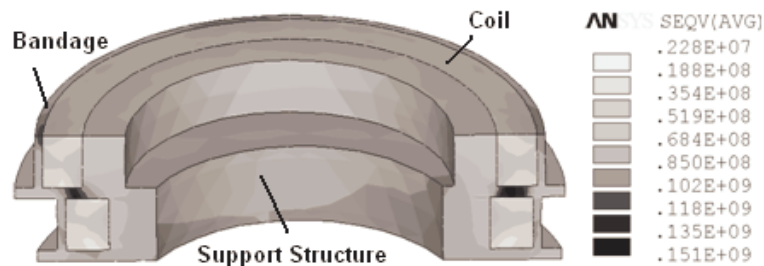


Fig. 4. Stress distribution in the model and its cross-section.

A Finite Element Model (FEM) was used to simulate the forces for a single double pancake. The inner SS 304 support ring has 10 mm radial thickness, and the outer SS 304 bandage has 2 mm radial thickness. The Lorentz forces are 40 kN in the transverse direction, trying to straighten the shifted coils, and 76 kN in the axial direction, trying to pull the coils closer. Fig. 4 shows the stress distribution in the model. The maximum stress in the coil is 67 MPa, and 151 MPa in the SS 304 support structure. Note that the degradation stress for YBCO tape is ~ 700 MPa, and the yield stress for SS 304 at 4.2 K is ~ 500 MPa.

2.3. Fabrication

To wind the double-pancake coils continuously, two spools of YBCO tape were connected by soldering the ends of both spools to a 12 mm \times 28 mm YBCO tape section. This forms the inner splice of the double pancake. The inner splice is glued into the slotted surface of the support ring. Once the splice is secured, one spool is clamped to the support structure while the second spool is mounted on the tensioner (Fig. 5). The winding system is comprised of five pulleys, allowing one to co-wind the YBCO and the Kapton insulation and adjust the alignment. After winding the first turn, a G-10 spacer is glued on the top of the inner splice area. The spacer compensates the flattened region of the support ring that was required to make the splice (Fig. 6). During winding (excluding the first turn) a tension of 133 N (30 lbs) was applied to the tape. After 57.5 turns, glue was applied to both the Kapton and the YBCO and one more turn was completed. Wind another half turn for the outer splice and cut the YBCO tape. Put spool 1 on the tensioner to wind the second coil in the same way.

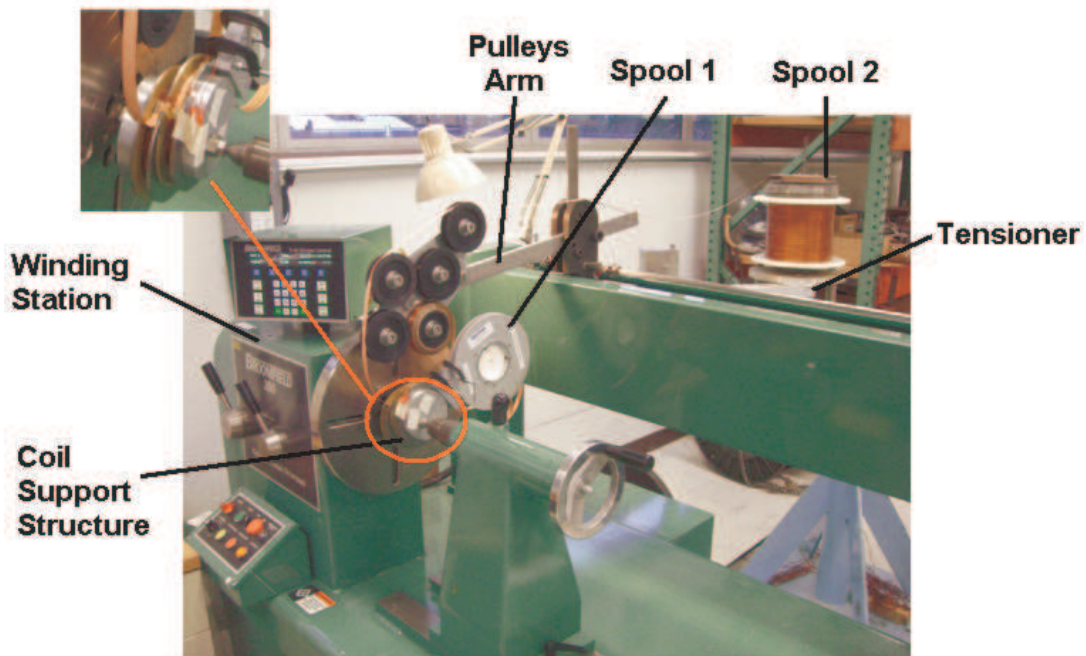


Fig. 5. Coil winding setup.

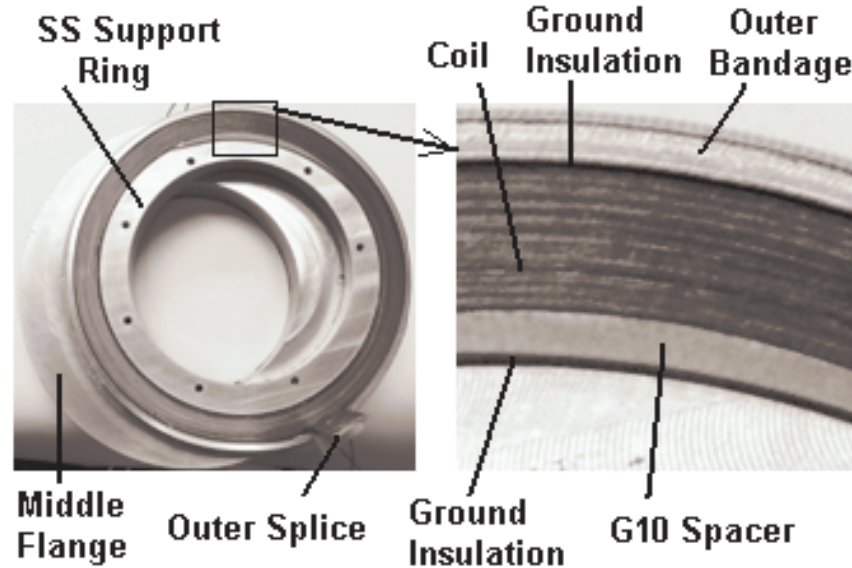


Fig. 6. Side view of one double-pancake model

The outer splice was made by soldering a 12 mm × 35 mm section of YBCO tape at right angles to each coil. Ground insulation and a support bandage were wrapped around the outside of the YBCO coil. Multiple layers of Kapton tape were used for ground insulation. Outside of the ground insulation 16 turns of (0.127 mm thick, 12.7 mm wide) stainless steel (SS) tape were wound as a support bandage. Finally, two turns of glass cloth electrical tape were wound outside the SS tape, and epoxy putty was used to hold the electrical tape position.

A. Insulation

For turn to turn insulation 0.05 mm thick, 12.7 mm wide Kapton is used to insulate the 0.1 mm thick, 12 mm wide YBCO tape. Each turn of the coil has one layer of the Kapton co-wound at the bottom of the superconductor, giving the packing factor of the coil about 66.7%.

For ground insulation, there are 10 turns of 0.05 mm Kapton on the top of the support rings, and another 5 turns of 0.05 mm Kapton on the top of the coil. The support side flanges are insulated by using 0.5 mm G-10 flanges glued with pieces of 0.025 mm Kapton sheet.

B. Splicing

Both coils of the double pancake are electrically connected through a piece of YBCO tape (12 mm × 28 mm) that fits into the inner splice recess. Each coil is connected to the current lead through a piece of YBCO tape (12 mm × 35 mm) which is fit in the outer splice slot. The piece of YBCO tape for the outer splice is also designed as the connection between two double-pancake units.

The splice performance is critical and may be the limiting factor in magnet performance. All splices are made by matching YBCO side of one tape to the YBCO side of the other. This avoids the known issue of the resistance being higher if one uses the configuration where the hastelloy is between the YBCO layers. The composition of the YBCO tape is shown in Fig. 7. Two splice samples were made using Sn63%Pb37%

(eutectic) solder, and tested in liquid Nitrogen. The measured splice resistance was less than 40 nΩ in both cases. Fig. 8 shows the voltage-current curves of the splices recorded during the test. Quench happened at about 310 A, and there is 6% degradation on the splices if I_c of the YBCO tape is assumed as the constant which is 330 A along the entire spool of superconductor.

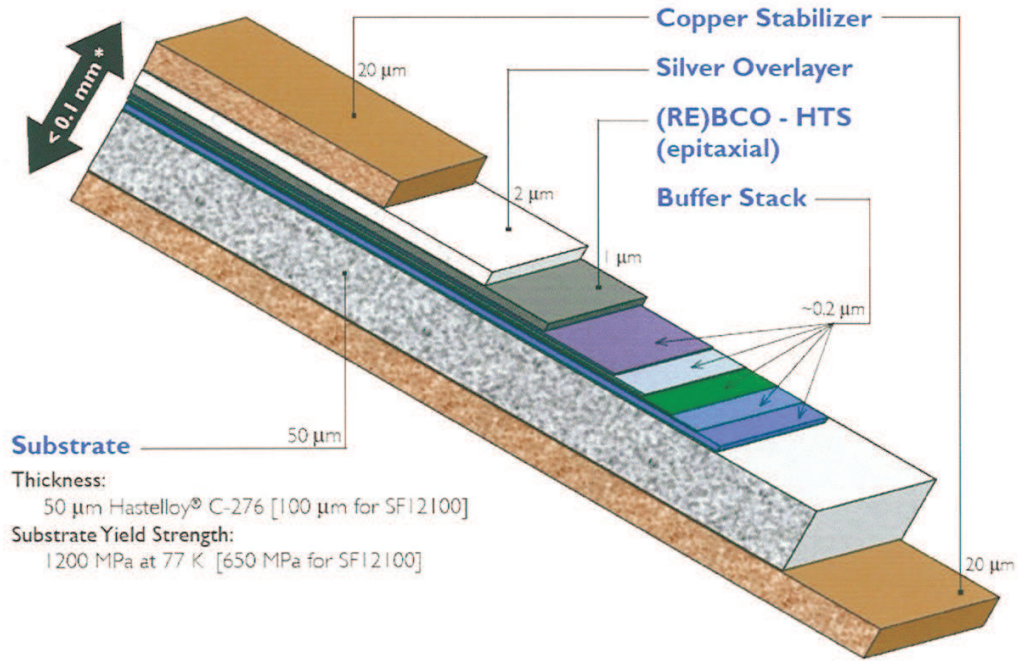


Fig. 7. The Composition of the YBCO Tape

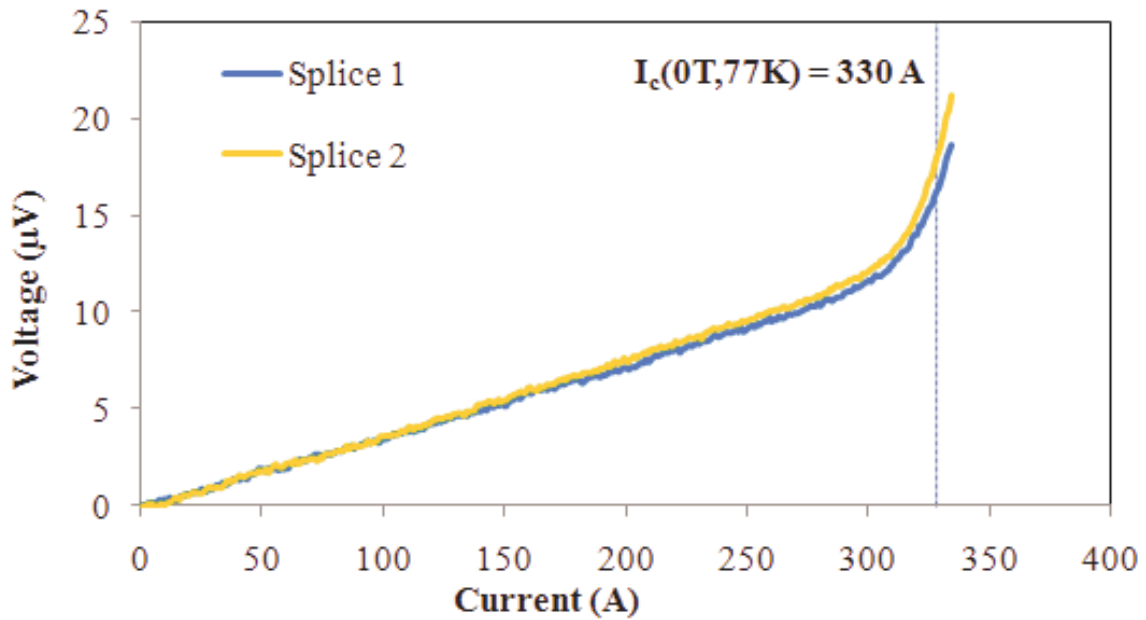


Fig. 8. V-I curves at 77 K for the splices.

2.4. Voltage Tap, Current Leads and Pre-test Electrical Measurements

The map of voltage taps to monitor the voltage vs. current on different sections of the magnet is shown in Fig. 9. VT1 and VT2 were soldered onto the inner splice. VT3 and VT4 were soldered onto the outer splices. VT5_QD and VT6_QD were soldered onto the turn before the last turn of each coil.

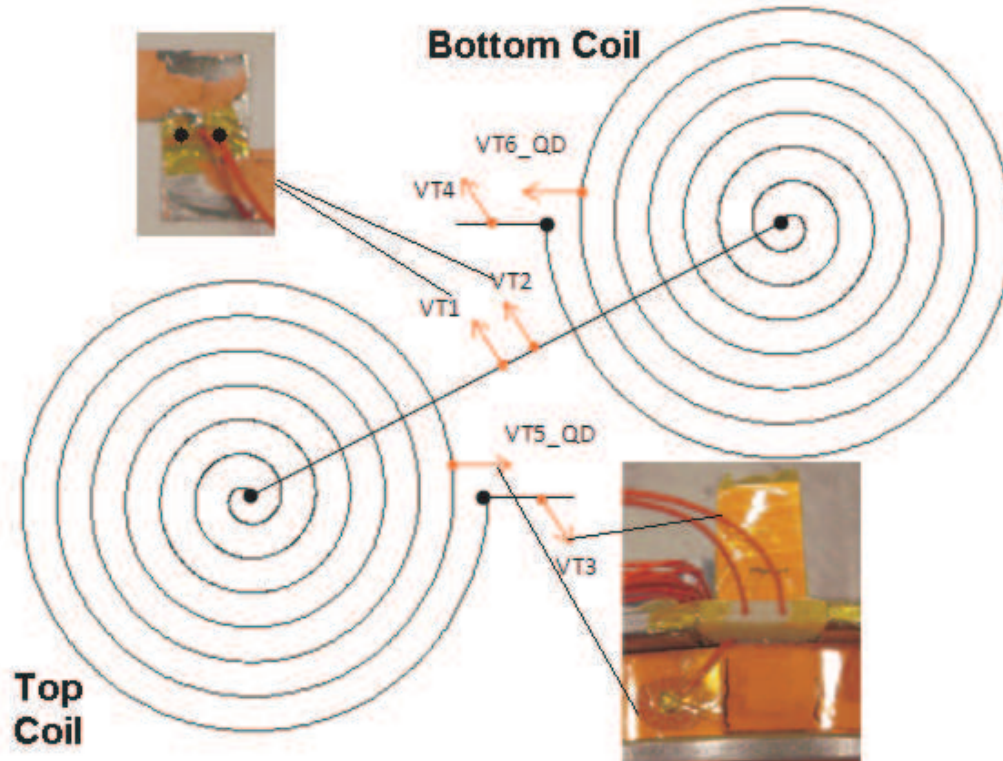


Fig. 9. Map of the Voltage Taps

To test the coils at 4.2 K (with a ~1.4 kA predicted quench current), two pieces of NbTi wire were soldered to the outer splice of each coil as the current leads. One end of the wire was wound into spiral shape to increase the contact surface area and then soldered to the outer splice. A G10 presser was assembled to provide support. Three pieces of 1 mm diameter copper wire were twisted with the NbTi wire to increase the rigidity of the leads. The other end of the wire was soldered to the probes concentrated current lead. Fig. 10 shows the current leads soldering process.

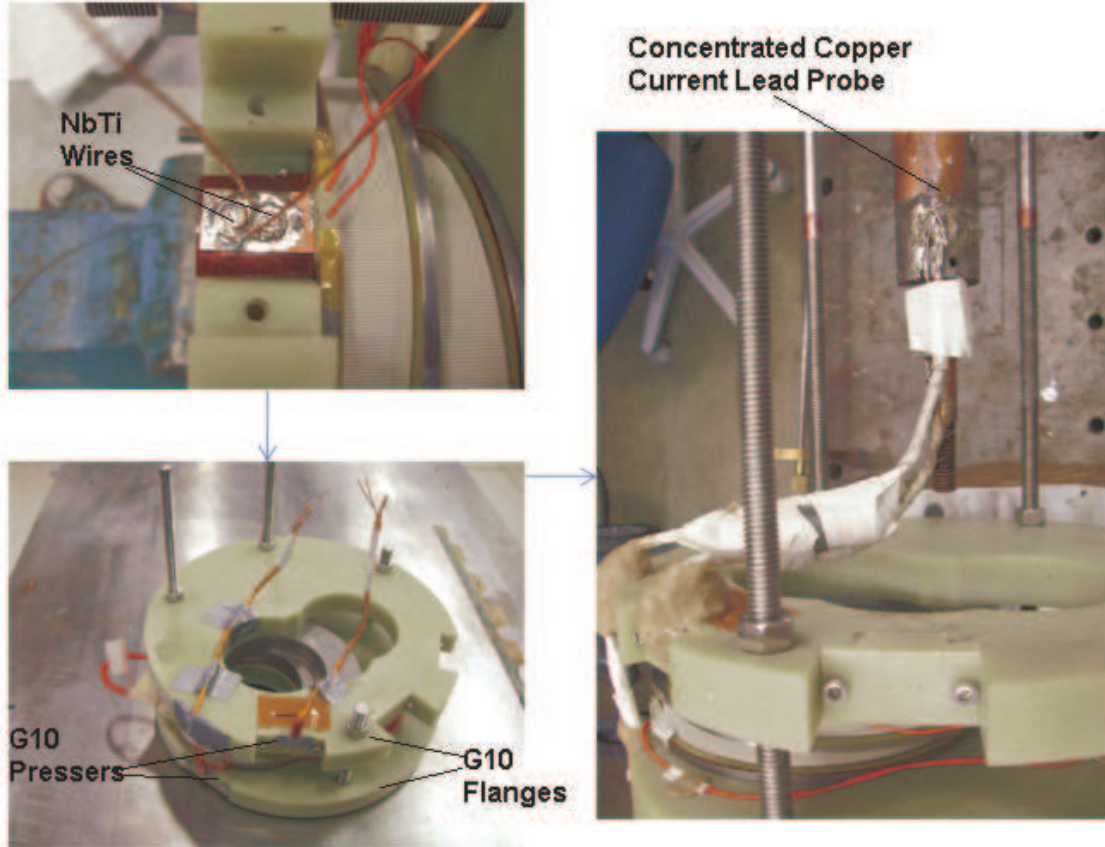


Fig.10. Soldering NbTi Wires as Current Leads

Magnet inductance, resistance, and Q value were measured. A high potential test (hipot) from coil to ground was performed to check the insulation. The measurement results are shown in Table 3. For quench protection, due to the low inductance and stored energy it was determined that an external dump resistor was not required, a concentrated current lead with a resistance of 1.6 mΩ would be a suitable substitute for an external dump resistor during the magnet excitation. (A more careful study on this subject was done for the next improved model, which will be shown later in this note.)

Table 3. Pre-test Electrical Measurements

Magnet Inductance	100 Hz 1 kHz	Ls1 = 617.76 μH, Ls2 = 634.12 μH Ls1 = 397.14 μH, Ls2 = 408.54 μH
Magnet Resistance		R1 = 0.684 , R2 = 0.681
Q value @ 100 Hz @ 1 kHz		Q1 = 0.19, Q2 = 0.20 Q1 = 0.77, Q2 = 0.78
Hipot Test: Coil - Gnd		1000 Volts, I < 0.1 μA

3. Test Overview and Results

3.1. Test Overview

The magnet testing was performed using a new dewar from Oxford Instruments. After an appropriate flange was designed and manufactured, and pressure vessel calculations were performed, permission to operate (silver sticker) the non-ASME vessel was obtained, following this pressure vessel tests were done.

For testing in the dewar, the double pancake model was assembled and clamped between two G10 plates that attached to the top flange through four SS rods. After measuring the magnetic field at 1.5 A at room temperature, the whole testing probe was inserted into the dewar, shown in Fig. 11.

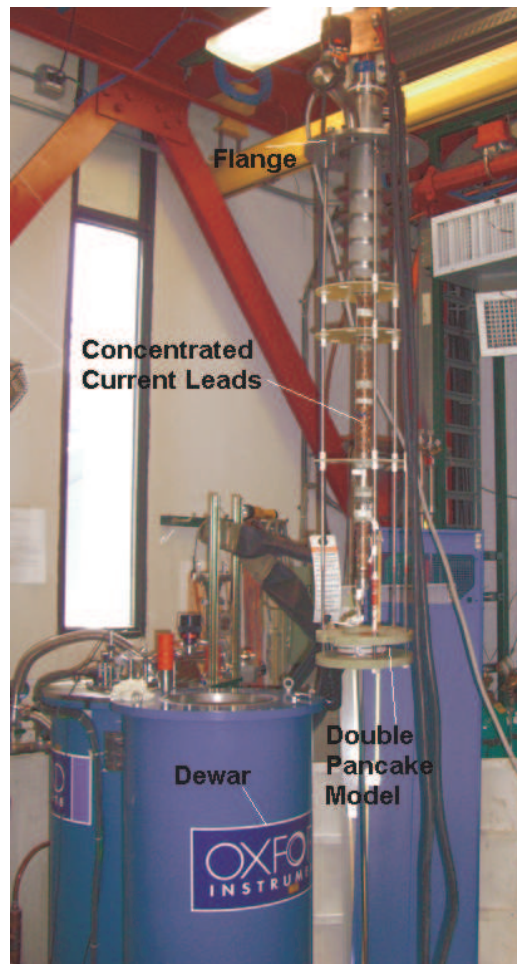


Fig.11. Final Assembly into the Testing Dewar

In order to test up to the 1.4 kA predicted quench current two Agilent 6680A (0-3.5 V, 0-1000 A) power supplies were used, when operated together they can provide 2kA. A National Instruments NI-PCI 6289 18 Bit 500Ks/second DAQ Card was procured and installed for data acquisition. Additionally, a National Instruments SCXI-1125 8 Channel Analog input channel 4 Hz, 10 KHz configurable low pass filter was used for signal

conditioning. A current ramp routine was designed to minimize current step sizes using 5-50 ms time steps.

Based on the voltage taps inside the magnet, the six data acquisition channels listed in Table 4 were used to monitor the voltage as the current was ramped. Due to the very low quench propagation velocity of YBCO tape, it is inadequate to use a conventional quench detection voltage limits to protect the magnet. In this and subsequent tests, the current was automatically stopped at voltage levels that are much lower than the critical voltage. Once the transition of the V-I curve was confirmed, the power system was stopped manually. One problem happened during the beginning of the test that the noise level in Channel 1 and Channel 2 reached 300 μV , higher than the threshold, so the signal was then bucked between these two channels, reducing the noise level to 5 μV .

Table 4. Details of Data Acquisition Channels

Channel #	Section based on Voltage Tap	Description
1	VT1-VT5_QD	Top coil: inner splice + 57.5turns
2	VT2- VT6_QD	Bottom coil: inner splice + 57.5turns
3	VT3-VT5_QD	Top coil: last turn + outer splice
4	--	Current lead (+) to Current lead (-)
5	VT4-VT6_QD	Bottom coil: last turn + outer splice
6	VT3-VT4	Two Coils

3.2. Field Measurement at Room Temperature

The magnetic field of the model was measured at room temperature. The sensor located at the end of the probe was placed at the center of the bottom coil, shown in Figure 12. The measurements are shown in Figure 13, which are consistent with the results calculated from the simulation.

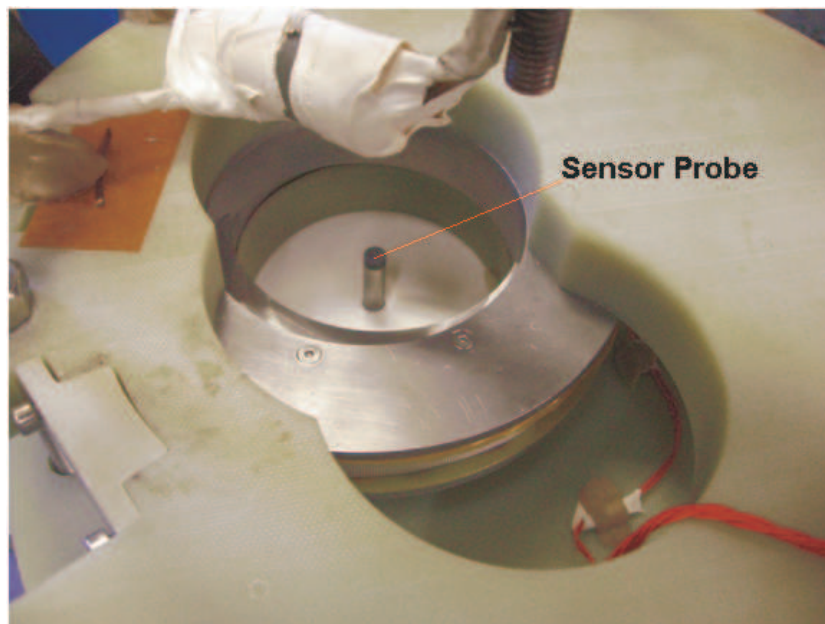


Fig. 12. Magnetic Field Measurement Setup

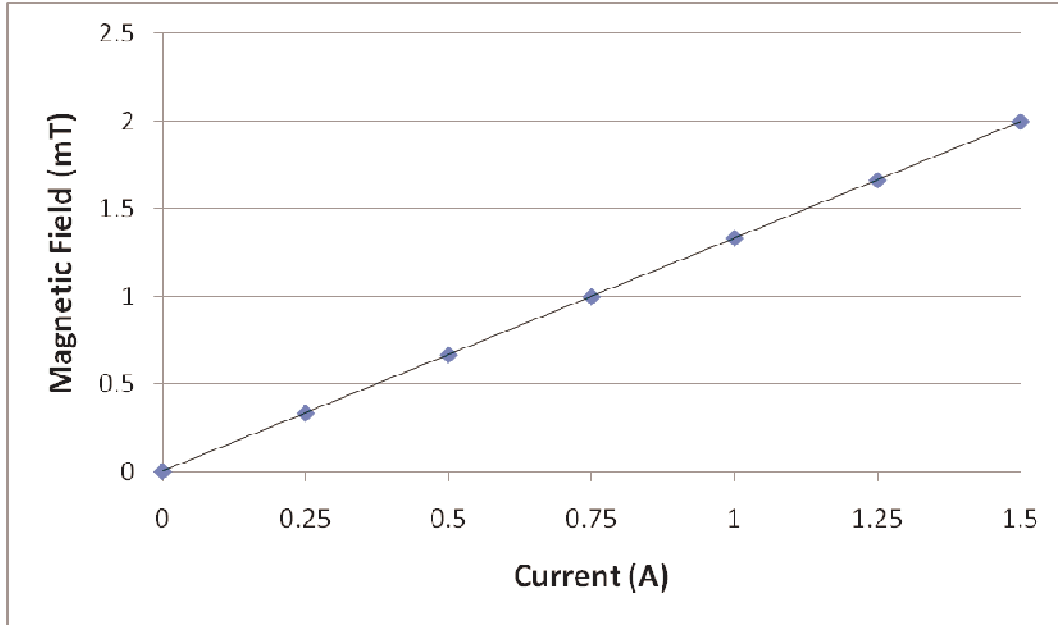


Fig. 13. Magnetic Field Measurements at Room Temperature

3.3. Magnet Performance at 4.2 K

The first double pancake was tested in helium using the aforementioned probe and dewer setup. The test was performed three times at the same ramp rate 0.5 A/s. The signal shown in Figure 14 was the bucked signal of the two coils (subtracting Channel 1 from Channel 2). All the quenches happened in the bottom coil due to the negative signal, at around 285 A, 20% of short sample limit at 4.2 K.

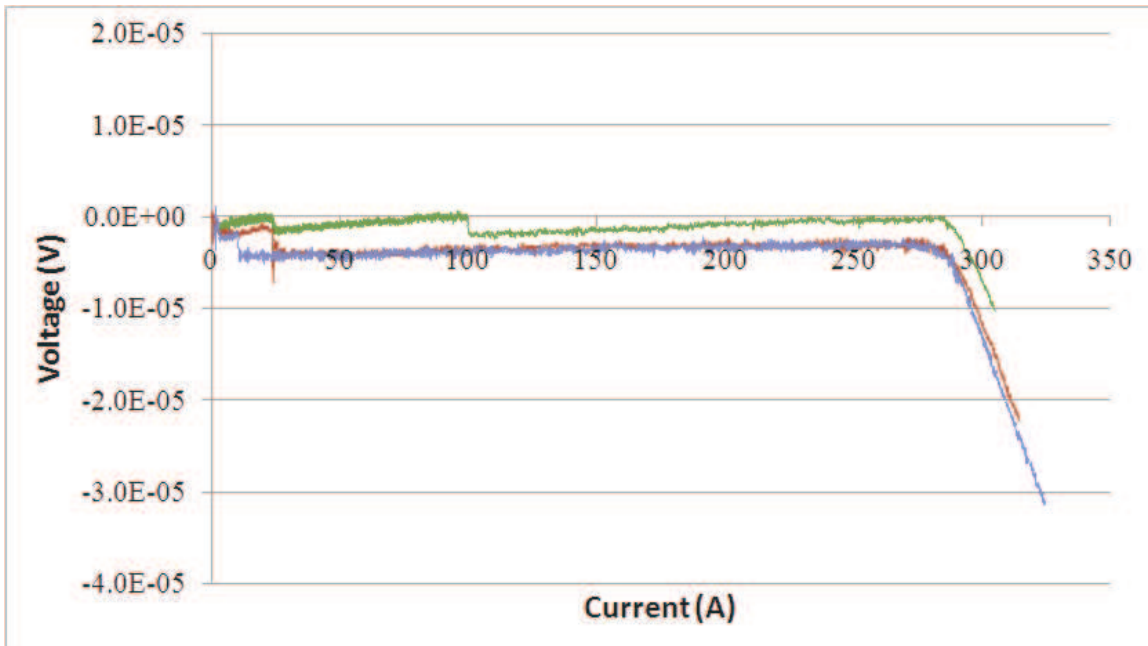


Fig. 14. Quench Started Earlier during the Test at 4.2 K

To get more information about the quench, an additional test was performed. The quench diagnostic test involved pausing the power supply at different current during the quench to let the system respond with the current held constant. The results are shown in Figure 15. The voltage signal remains at the same level when the current is paused indicating the quench was not due to the mechanical defect. If the quench was initiated by a mechanical effect one may reasonably expect the system would recover in the absence of the effect. Moreover, a ramp rate study at 1 A/s, 2 A/s and 5 A/s was also performed. The transition happened at ~285 A for all three cases, shown in Figure 16. Due to the limitation of the power supply, the ramp rate cannot go higher than 5 A/s. The results indicate that one or both of the coils suffered degradation during the fabrication process. The degradation location and its reason were studied and discussed in the following.

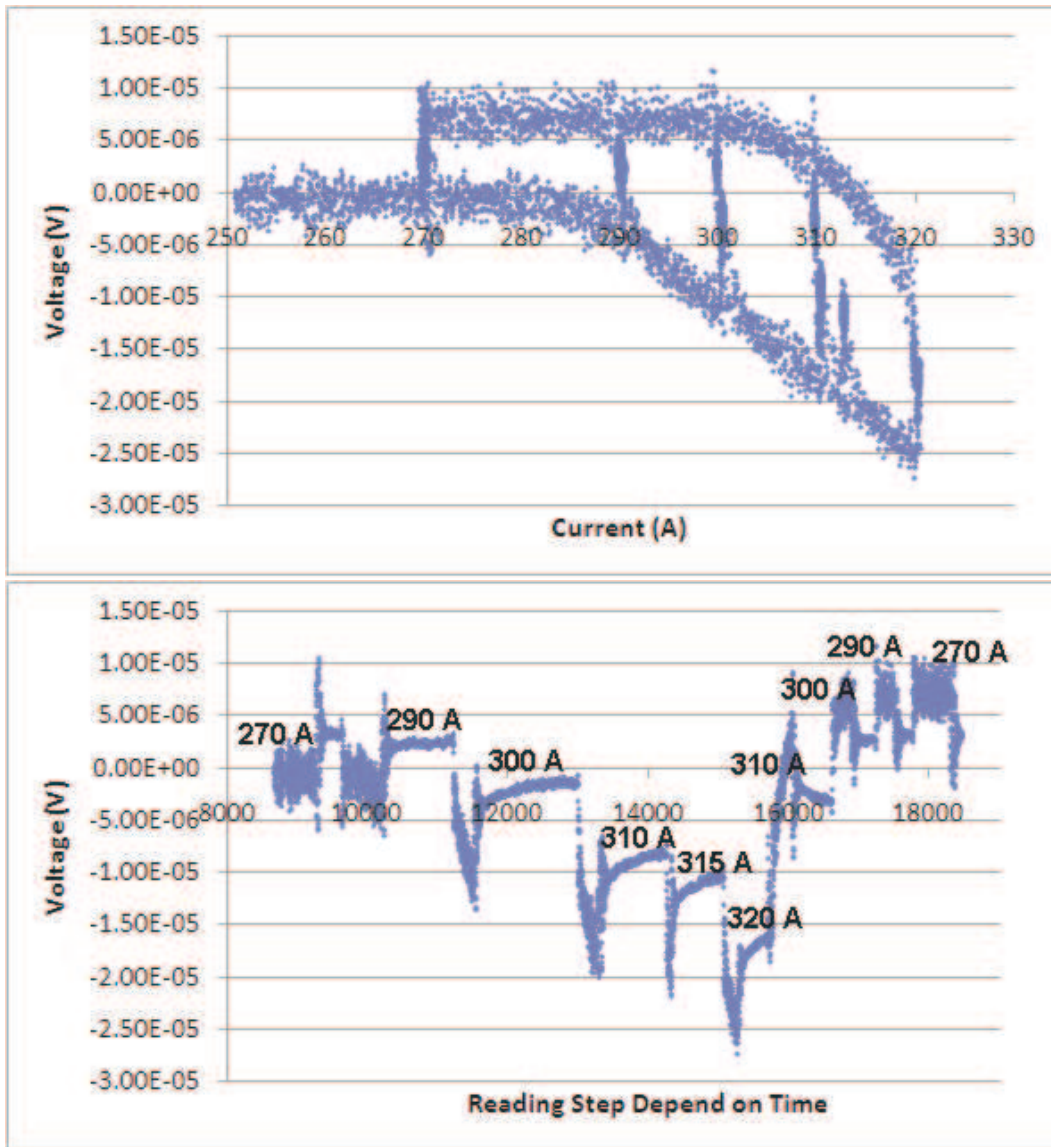


Fig. 15. Pause during Quench

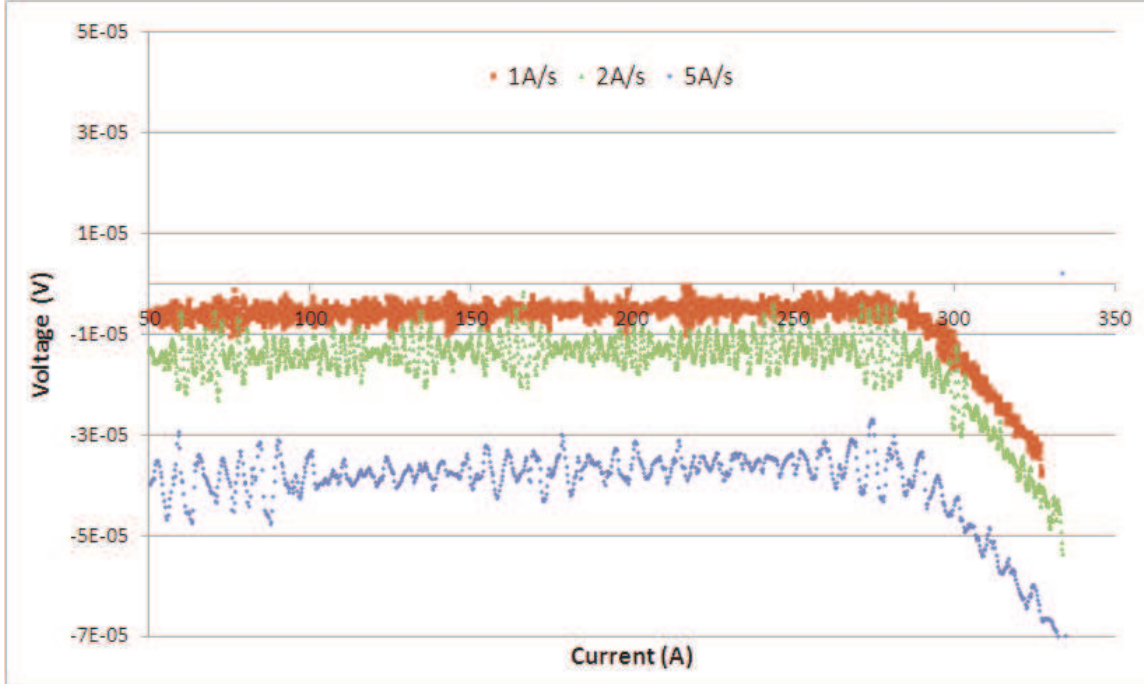


Fig.16. Test at Different Ramp Rate

3.4. Splice Resistance

There are four soldered splices in the model, two inner splices and two outer ones. The resistances of the outer splices were measured during test at 4.2 K, shown in Figure 17. The resistance of the top coil outer splice is 484 nΩ, much higher than the average resistance ~40 nΩ of the splice samples, however, this was not the cause of the quench in the bottom coil.

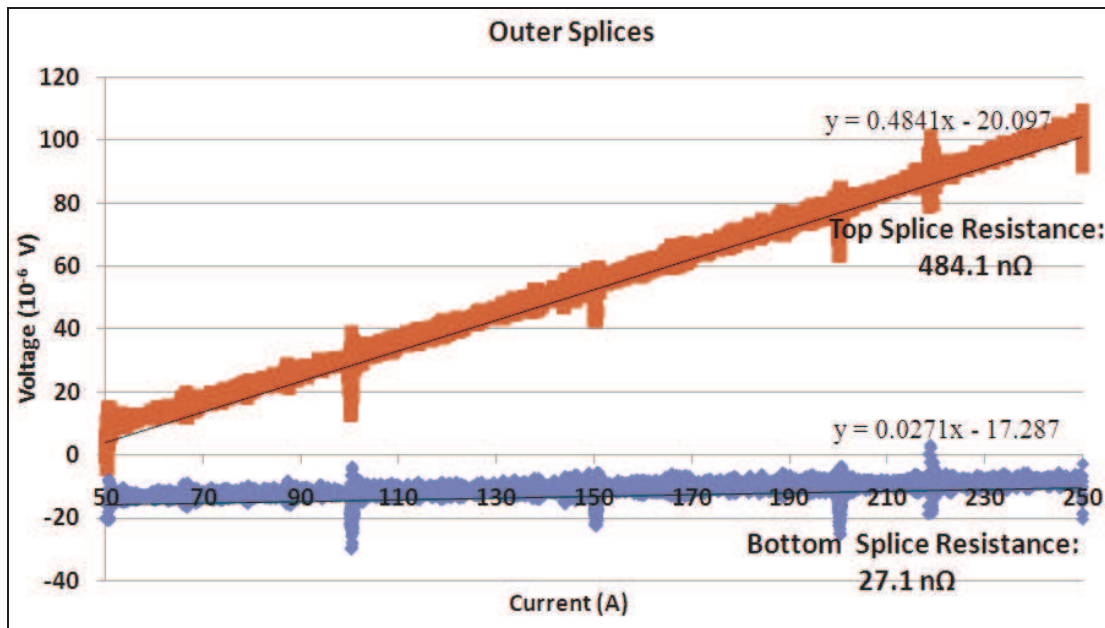


Fig. 17. Resistance Measurements for Outer Splices

4. Post-Test Inspections and Study

There were several concerns about using super glue and cooling the magnet down too quickly. The super glue applied on the surface of the tape during winding and fast cooling rate when cool the magnet from room temperature to 4.2 K may degrade the conductor in cold test due to different thermal shrinkage of materials in the magnet. In the post-test study, the location and the reason of the degradation were found and discussed.

4.1. Inspection

YBCO HSM01 was removed from the test facility, the side flanges were disassembled so that both coils can be visually inspected. The outer splice of the top coil was found to be badly deformed. The deformation resulted in the high observed resistance, shown in Figure 18. The top G10 flange was attached to the coil only by tightening nuts in four rods, which needs to be improved for the next model.

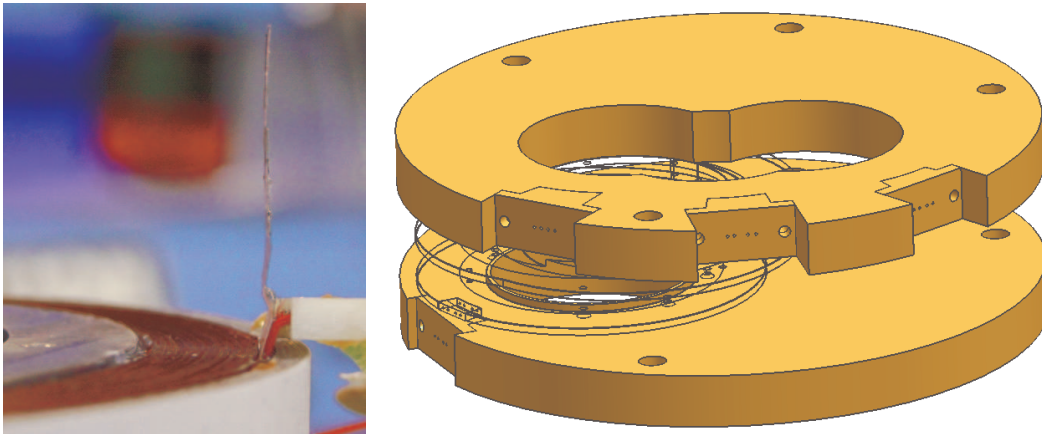


Fig. 18. Deformation on the Outer Splice of Top Coil

The coil was observed under the microscope, shown in Figure 19. Too much super glue was used when put the G10 spacer on to the inner splice area, causing bending of the inner most turn of the coil, shown in the right picture. Controlling the amount of the super glue is strongly suggested for the next model if super glue is still used.

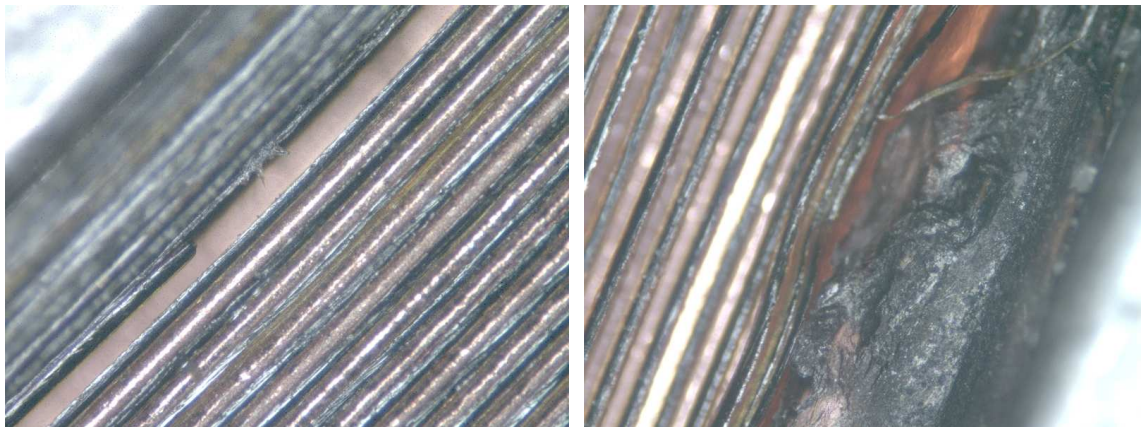


Fig. 19. Coil Observation under the Microscope

4.2. Degradation Location and Reason

YBCO HSM01 showed significant degradation in the 4.2 K test. A 77 K test was performed on the double pancake, which showed consistent degradation. For the 77K test, copper leads made of multilayer copper shims were soldered to the outer splices, replacing the NbTi wires. During the test, the data was recorded 2.5 s after the current is ramped up each time, so that the high level noise in the signal of both coils was avoided. The long data sampling rate was considered acceptable in this test since the current is much lower, the results are shown in Figure 20. The bottom coil quenched at around 28 A. The short sample limit at 77 K is about 100 A.

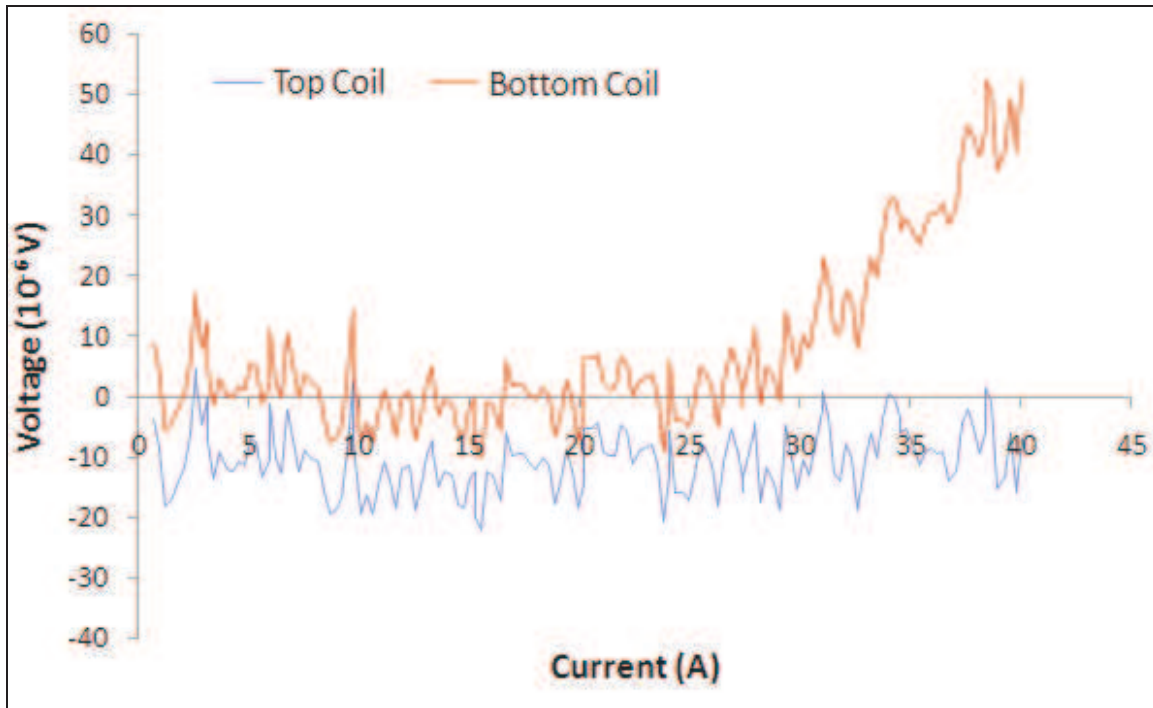


Fig. 20. YBCO HSM01 Test at 77 K

The first step, two more voltage taps were soldered to the last two turns of the bottom coil where the super glue was applied. The test result indicated that the degradation was not in this area. There is enough pre-stress from the winding tension and the outside bandage that will prevent the separation of two turns during cooling down. The second step, the bottom coil was unwound and rewound. During rewinding additional voltage taps were inserted, the additional voltage taps are mechanically pressed due to the winding tension. Following the rewinding the double pancake was retested at 77 K, the location of the degradation was narrowed down to the inner splice plus the conductor under the G10 spacer. The third step, both coils were unwound, and the inner splices were cut and tested at 77 K. The test result is shown in Figure 21. The degradation location was pinpointed at one edge of the inner splice.

Two possible reasons for the inner splice degradation were suspected. The first one is the splice soldering temperature. The soldering temperature should be kept below 250 °C (recommended by Superpower), however, for the initial model there was no temperature

control during splice soldering. The second concern was the splice area design and winding technology, shown in Figure 22. It is possible that high stress could be applied to the edge of the splice during the winding.

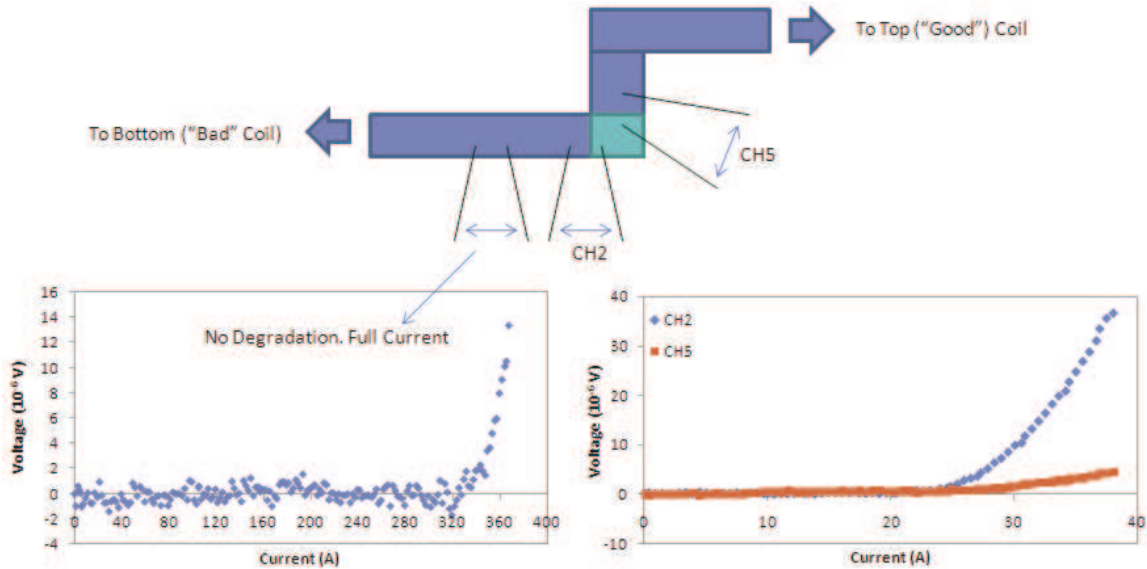


Fig. 21 Inner Splices Test at 77 K

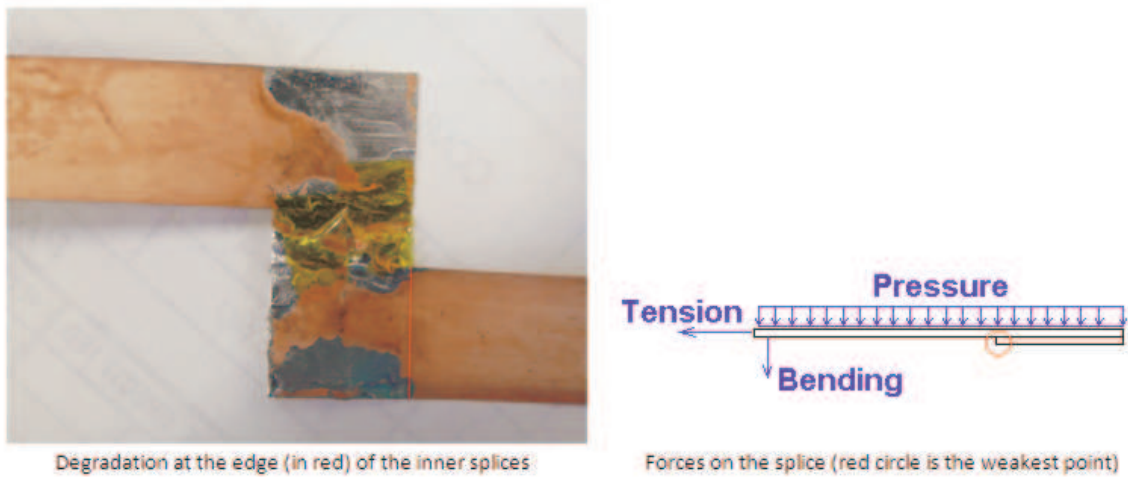


Fig. 22. Possible Reason for the Degradation: Stress Concentration

Two sets of inner splice samples were soldered by two different technicians. Technician 1 controlled the soldering temperature and technician 2 did not control the soldering temperature (higher than 250 °C). Four inner splice samples were tested at 77 K, following this benchmarking, the splices were bent and pressed during the coil winding process and retested at 77 K. No critical current ($I_c(77K,SF)=360A$) degradation occurred in any of the samples. However the resistance of the splice from Technician 2 is higher than the one from Technician 1, which is shown in Figure 23. To avoid the unexpected degradation, controlling soldering temperature is highly recommended.

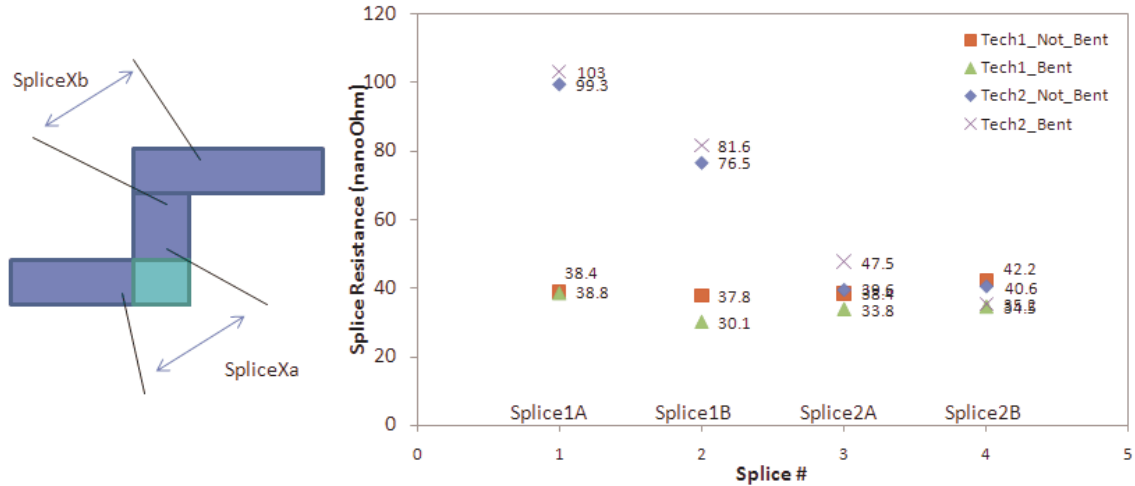
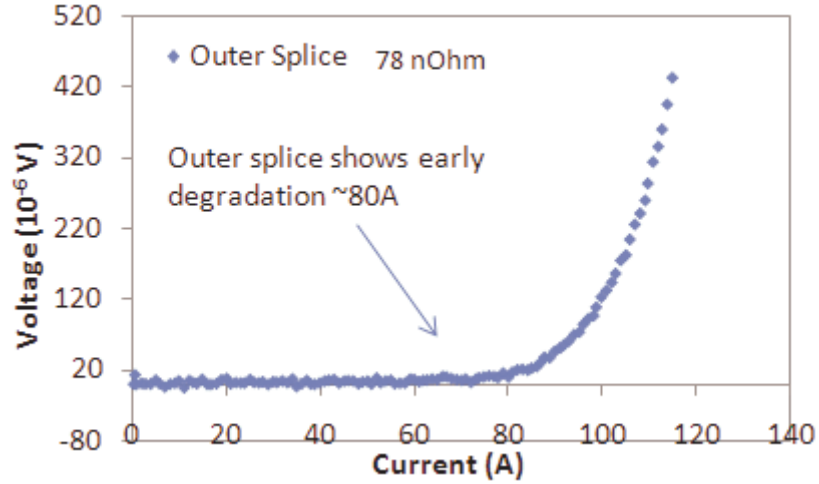


Fig. 23. Resistance of the Inner Splice Samples

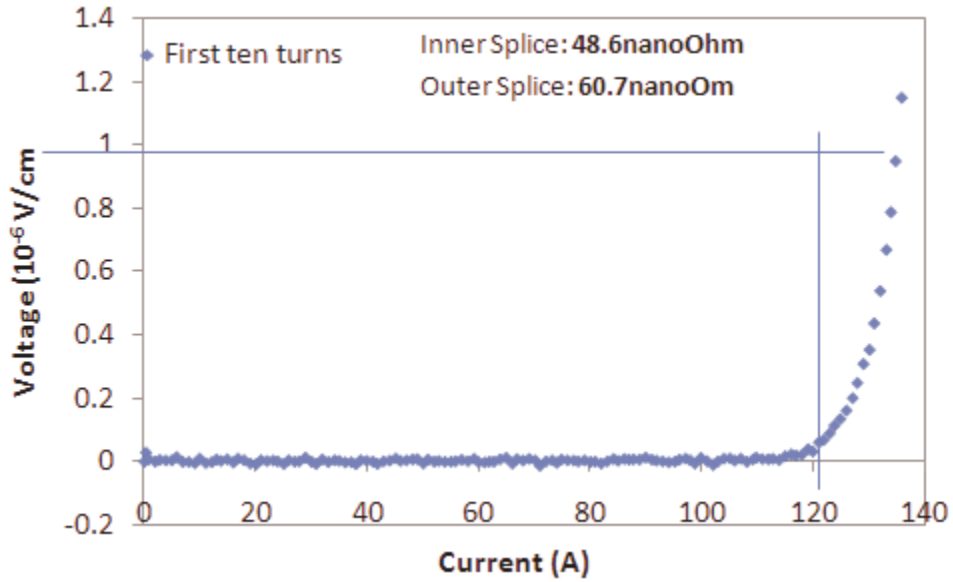
4.3. Single Coil Winding and Test

The YBCO tape used in the model was wound and unwound several times. To verify the tape’s performance, the two coils needed to be independently testable. The top and bottom coils were re-wound and copper leads were soldered to YBCO inner and outer splices. The water cooling system was used during the soldering to reduce the heat transferring into the coil. The top coil was tested first in liquid nitrogen. Inner splice showed an acceptable 61 nΩ resistance and no degradation, whereas the outer one, despite the low resistance, started to show voltage around 80A, ~65% of SSL. The bottom coil was then tested. No degradation occurred in any of the splices. The test results for both coils are shown in Figure 24. Controlling soldering temperature for splices and copper leads can improve the coil performance.

From the post-test study, the degradation location was found. It was determined that soldering temperature was the most likely reason for the degraded performance. Soldering splices by hand increases the chance of degradation (and can cause issues in terms of reproducibility). Additionally, it was found that the YBCO tape could be unwound and rewound ~10 times without introducing significant or measureable performance degradation.



(a) Top Coil



(b) Bottom Coil

Fig.24. Top and Bottom Coil Test Results at 77 K

5. YBCO HSM1.1 Fabrication and Test

While the basic winding procedure remained the same, several improvements were introduced into the soldering component of the fabrication procedure. The first improvement was the introduction of the soldering fixture to make the splices. This allows for control of pressure, temperature, and aids in reproducible splice production. The second improvement relates more to the testing procedure than the fabrication process. The G10 presser was replaced by a copper presser for the outer splice. This allows a pressure contact to be used for testing at 77 K and reduces the number of times the outer splice needs to be soldered. During unwinding and rewinding procedure, several turns of YBCO tape were lost, so there are 51 turns each coil for HSM1.1.

5.1. Splice Soldering Kit

To make splice soldering more reproducible, a soldering kit was machined using some existing aluminum parts, shown in Figure 25. Four bolts and springs are used to adjust the soldering pressure. 5 mil tin sheets were used as the solder. During soldering, the top plate is heated up, and the soldering temperature 200°C can be controlled by monitoring the temperature of the aluminum bar. Once it reaches 200°C, turn off the power and cool down the top plate by using pieces of cloth soaked in the water.

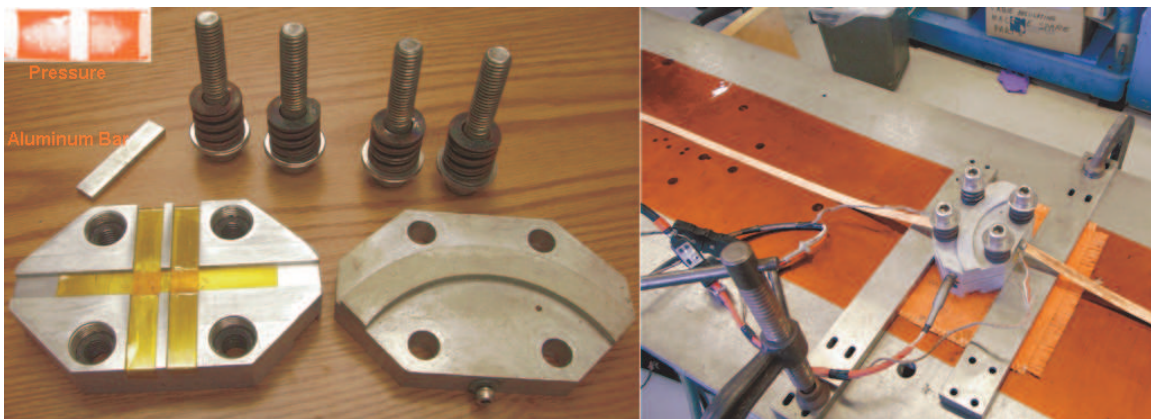


Fig.25. Splice Soldering Kit

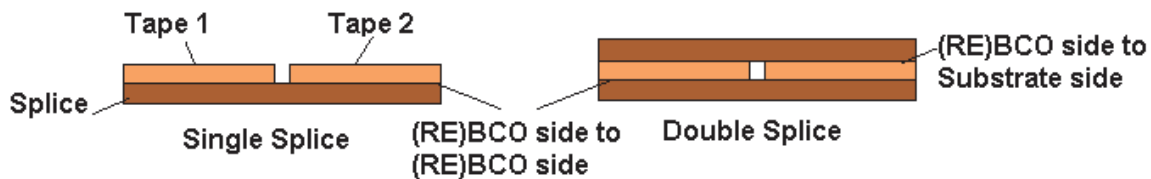
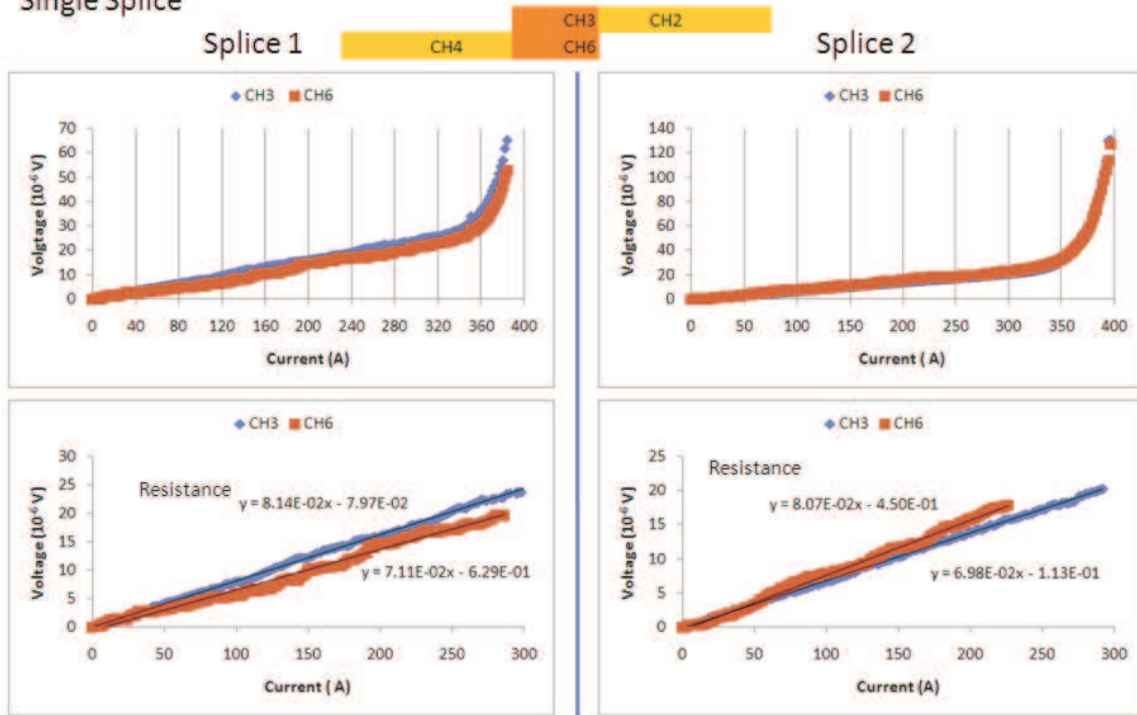


Fig.26. Sketch of Single and Double Splice

Several splice samples, including single splice and double splice shown in Figure 26, were made and tested. The results are shown in Figure 27. The critical current for the YBCO tape is in the range of 330 A ~ 360 A, due to conductor consistency. From the results, both single splice and double splice reached short sample limit. The resistance for each splice is in between 53nΩ and 89nΩ.

Single Splice



Double Splice

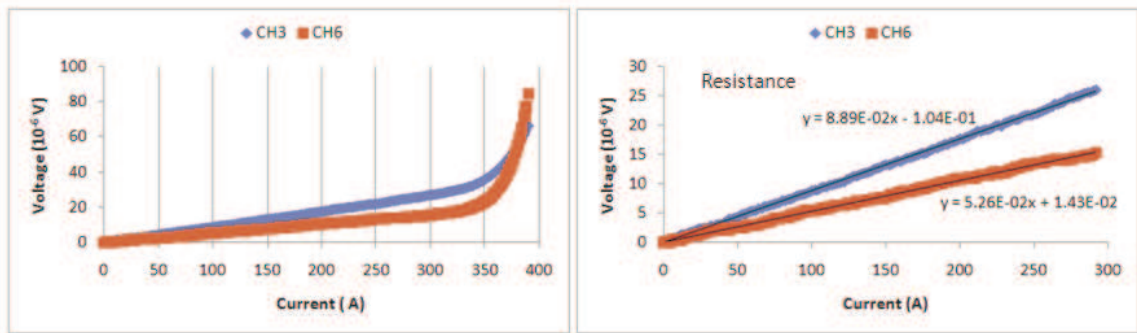


Fig.27. Test Results of the Splices Made by Soldering Kit

5.2. Copper Presser

G10 pressers were designed to support the outer splices for the first model and current leads were soldered to the splice to power the magnet, which damaged the outer splices. Therefore, copper pressers were machined, replacing the G10 pressers, shown in Figure 28. Two pieces of indium sheet were inserted in between the copper pressure and the outer splice to enlarge the contact surface, which can lower the resistance by one order of magnitude. The copper current leads can be soldered to the presser instead of the splice to protect the splice from soldering damage.

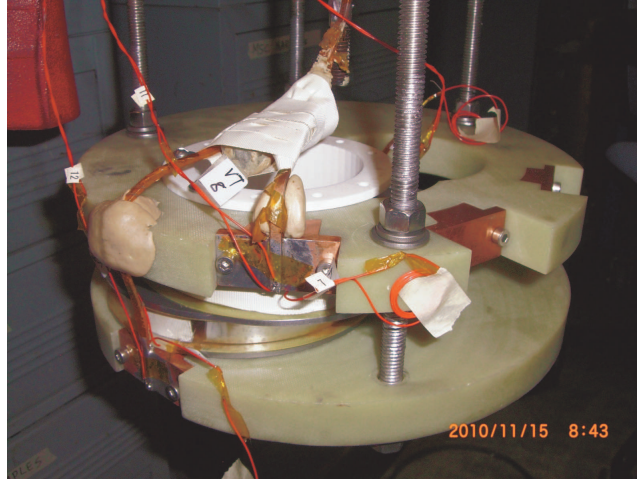


Fig.28. Copper Pressures Attached to the Model

5.3. Test Instrumentation and Pre Electrical Test

To monitor the model performance, 12 voltage taps were installed, and the map is shown in Figure 29. Voltage taps VT3-VT6 have a mechanical contact to the conductor, the rest were soldered. The electrical contacts for the voltage taps were checked, shown in Table 5. Voltage taps VT1-VT3 cannot be used due to the disconnection (no readings during the measurement).

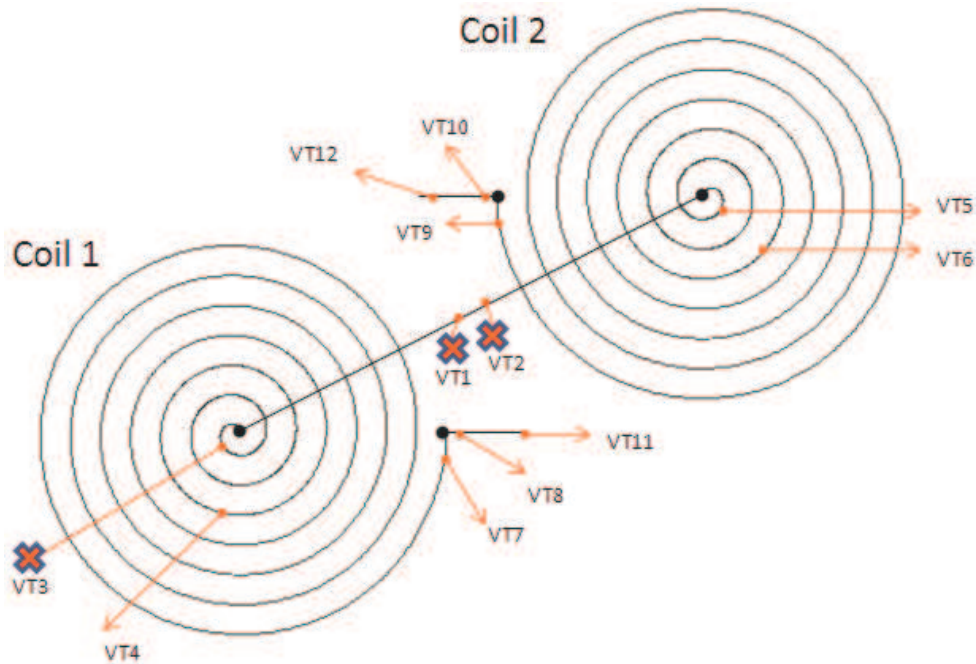


Fig.29. Map of Voltage Tap

Table 5. Pre-test Electrical Measurements

Magnet Inductance	100 Hz	1.425 mH
	1 kHz	0.704 mH
Magnet Resistance		1.32 Ω
Q value @ 100 Hz @ 1 kHz		0.64
		0.98
Hipot Test: Coil - Gnd		500 & 1000 Volts I = 0.014 μ A

5.4. Short Sample Limit

The nominal critical current of 12 mm YBCO tape at 77 K is 330 A. The expected current for HSM1.1 was limited by the field component that was perpendicular to the tape, and this perpendicular component is caused by the fringe field of the solenoid shown in Figure 30. Figure 31 shows the load line of the model across the I_c vs. B curves at 4.2 K (based on the measurements [15]) and 77 K (scaled down from the measurements taken at 4.2 K). The short sample limit of the model is 103 A at 77 K, and 1468 A at 4.2 K respectively.

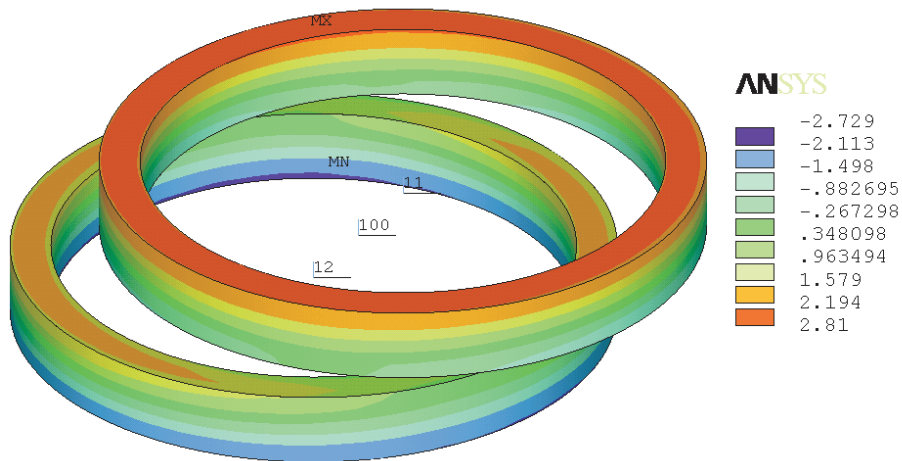
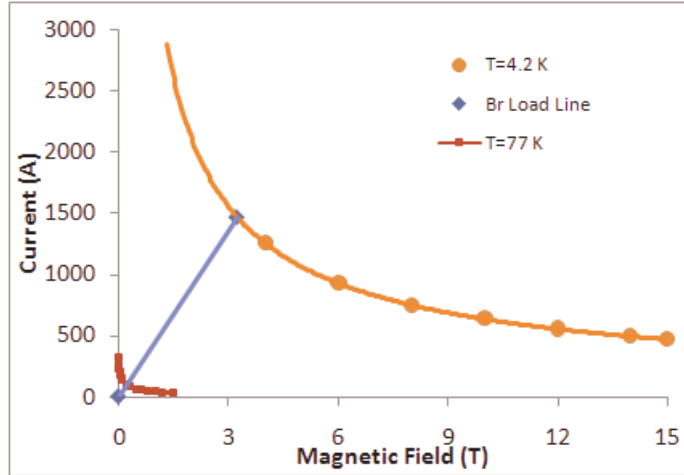
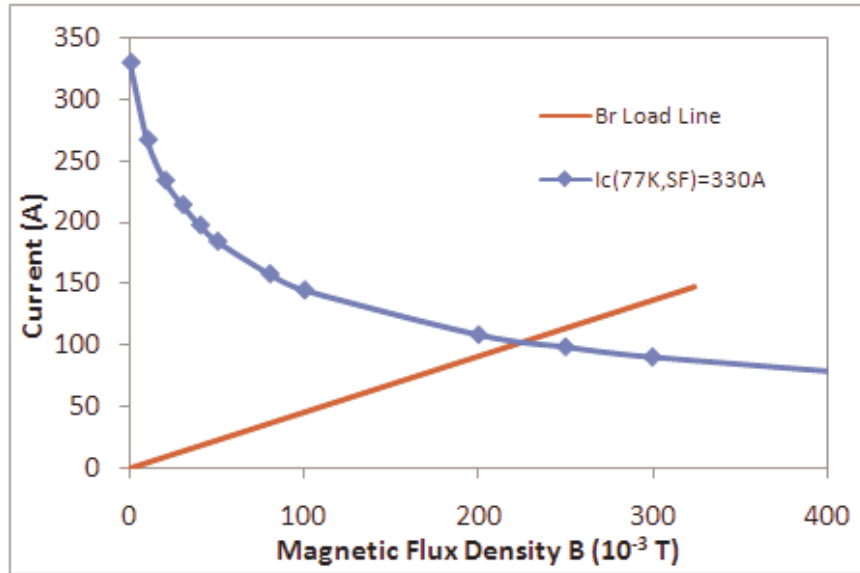


Fig. 30. Magnetic Field Radial Component Distribution (Perpendicular Field to the Tape)



(a) Model Load Line at 4.2 K and 77 K



(b) Model Load Line at 77 K

Fig.31. Current Short Sample Limit for YBCO HSM1.1

5.5. Test at 77 K

YBCO HSM1.1 was dumped into the cooler box filled in with liquid nitrogen. Six channels for the data acquisition monitored different portions of the model, shown in Table 6. The threshold for quench protection was set at less than 100 μ V. The test result is shown in Figure 32. The data were trimmed by subtracting the resistance components, shown in Figure 33. The transition started at 90 A, ~87% SSL, in the inner splices section. The total resistance in the two inner splices is 174 n Ω . The resistance of the outer splice is 61 n Ω in coil 1 and 148 n Ω in coil 2. The curves for both coils with slope in Figure 32 indicate that there was some resistance in the superconducting coil. After testing with a higher ramp rate, the slope of the curve became higher, which indicate that the current ramp rate was not constant and the voltage was generated by the inductance of the coil.

Table 6. Details of Data Acquisition Channels

Channel #	Section based on Voltage Tap	Description
1	VT8 to VT7	Coil 1: Outer splice
2	VT7 to VT4	Coil 1: Last turn to 6 th turn
3	VT4 to VT6	6 th turn of Coil 1 + inner splices + 6 th turn of Coil 2
4	--	Current lead (+) to Current lead (-)
5	VT6 to VT9	Coil 2: 6 th turn to last turn
6	VT9 to VT 10	Coil 2: Outer splice

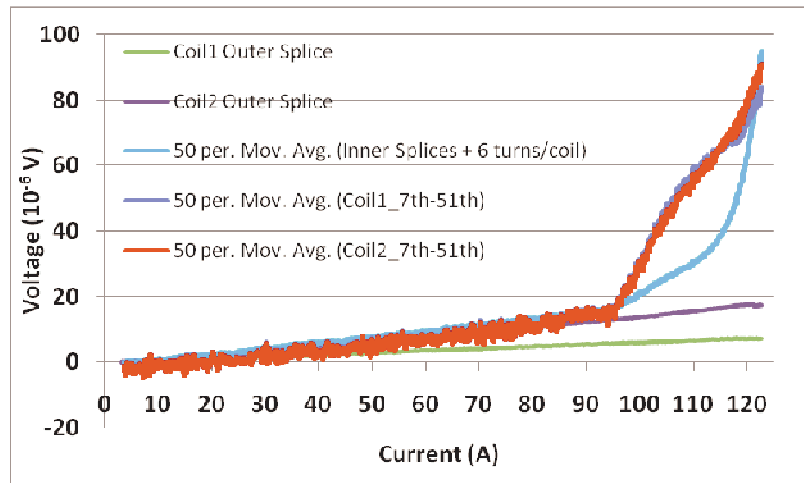


Fig. 32. HSM1.1 Test Results at 77 K

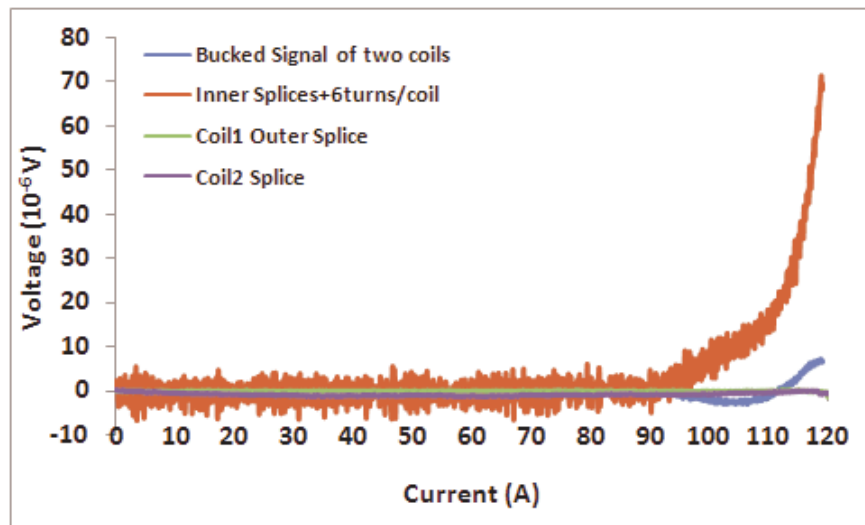


Fig. 33. HSM1.1 Trimmed Data Results

5.6. Quench Protection

Quench protection is the critical element to safely test the model at 4.2 K where the expected SLL is ~1.4 kA (the total stored energy is only around 1.33 kJ).

The Teslatron 2 test station in the SCR&D Lab is equipped with two power supplies Agilent 1000A 3.3 Volt operating in parallel for a total of 2000 A. The current is delivered to the load through four ERIFLEX flat cables for a total impedance of 0.5 mΩ, shown in Figure 33. The inductance of the model is about 1.5 mH.

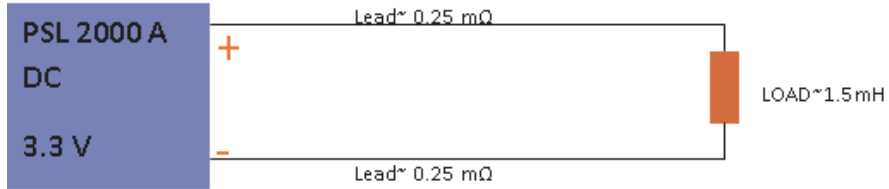


Fig. 33. Circuit of the Current Test Station Setup

To provide safe current decay time constant of ~1 s when testing the HTS helical solenoid, a resistance of 1.5 mΩ or more is required in series with the load and the capability to deliver a current to up to 1400 A (estimated short sample limit). Whereas the latter requirement is fulfilled by the 2000 A max current, the former would be met only with a resistor of at least 1 mΩ between the current leads and the load. The value of the resistance to be put in series is also limited by the max PS voltage as follows:

$$3.3 \text{ Volts} = R * 1400$$

$$R = 3.3 / 1400 = 2.35 \text{ m}\Omega$$

The requirements of the resistance (1 mΩ, 2 KW) are almost impossible to be fulfilled with a commercial resistor. However, they can be met by using four 15 feet long copper welding cables of 3/0 gauge with FLEX-A-PRENE isolation as resistors, and connected as shown in Figure 34.

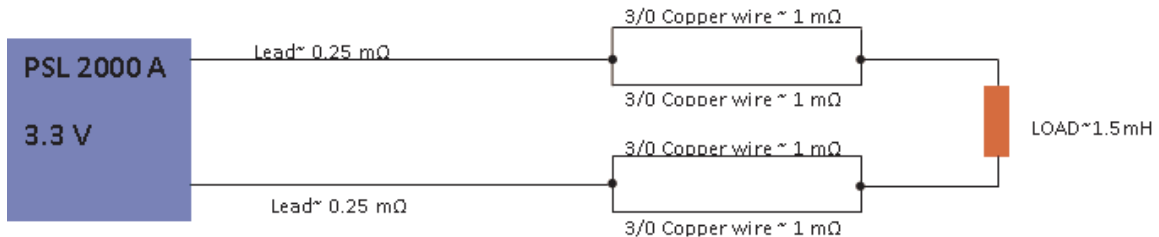


Fig. 34. Add Copper Cables as the Resistors into the Circuit.

Table 7. Cable Ampacity

SUGGESTED AMPACITY FOR WELDING CABLE

GAUGE	50'	75'	100'	125'	150'	175'	200'	225'	250'	300'	350'
#4	100	100									
#3	150										
#2	200	150	100	100							
#1	250/300	200	150		100						
1/0	350	250	200	150		100	100				
2/0	400/450	300	250	200	150		100	100			
3/0	500	350/400	300	250	200	150	150			100	
4/0	550/600	450/500	350/400	300	250	200	200	150	150		100

Table 8. Maximum Allowable Voltage and Temperature

CABLE	FLEX-A-PRENE®	VERI-FLEX
PROPERTIES		
Voltage:	600	600
Low Temp:	-50°C	-40°C
High Temp:	+105°C	+90°C
Durability:	Heavy Duty	All Purpose

The resistance of each cable is almost 1 mΩ and the ampacity from the cable company is shown in Table 7. The maximum allowable voltage and temperature of the cable to be used (FLEX-A-PRENE, heavy duty) are reported in Table 8. An extrapolated value of the ampacity (667A) for a 15 feet long cable is plotted in Figure 35.

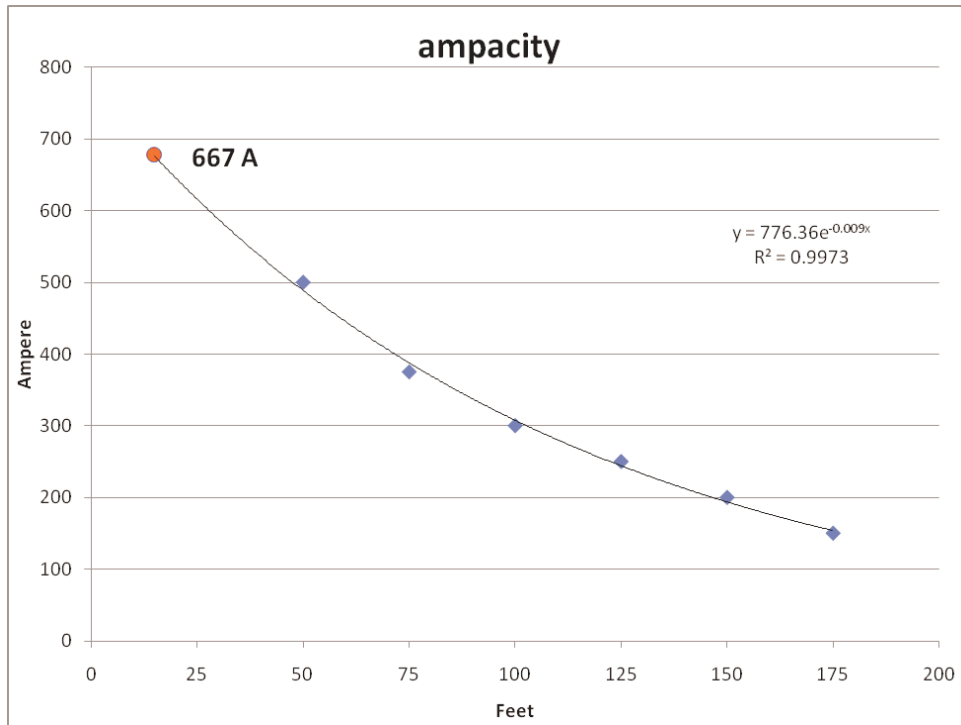


Fig. 35. The ampacity for a 15 feet long cable

A test of the four cables has been done in the SC R&D Lab in order to measure the max temperature and evaluate the possible hazards during the solenoid test. The cables have been connected and instrumented with 12 Type E thermocouples as shown in Figure 36. A current of 0.5 A/s has been ramped in the four cables and the temperature continuously monitored and acquired with a Keithley 2700 multimeter. A temperature limit of 90 °C, which is 15 °C below the max allowed cable temperature, has been set as threshold to shut off the power supply. As shown in Figure 37 and Figure 38, the max current reached 1.4 kA, which is the expected the short sample limit of the helical solenoid.

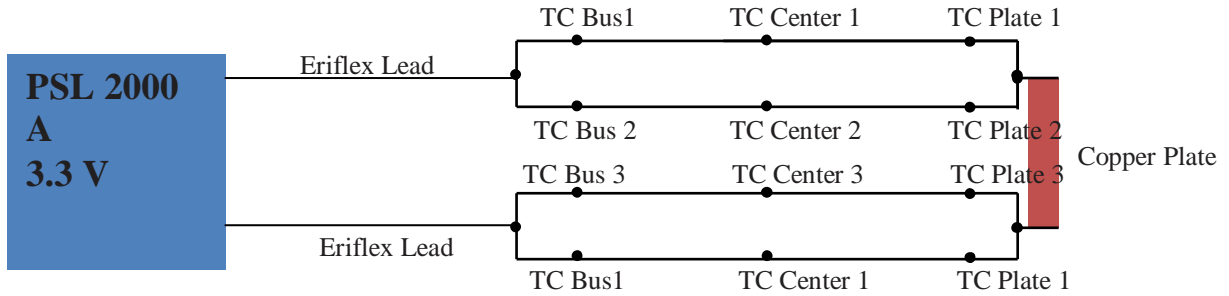


Fig. 36. Cable Test Circuit

According to the “Fermilab manual ES&H 5046 Low Voltage, High power Distribution systems” guidelines “*High currents, coupled with lack of adequate over current protection and/or undersized conductors, can lead to overheating of the conductors between source and load, thus presenting a fire hazard*”. As the test has shown, the risk of fire will be satisfactorily mitigated with the continuous presence of personnel during the test, the relative short time of the test (50 minutes) and, more importantly, with a continuous monitoring of the temperature along the cables and the automated shut off of the power supply when the temperature reaches the threshold of 90 °C.

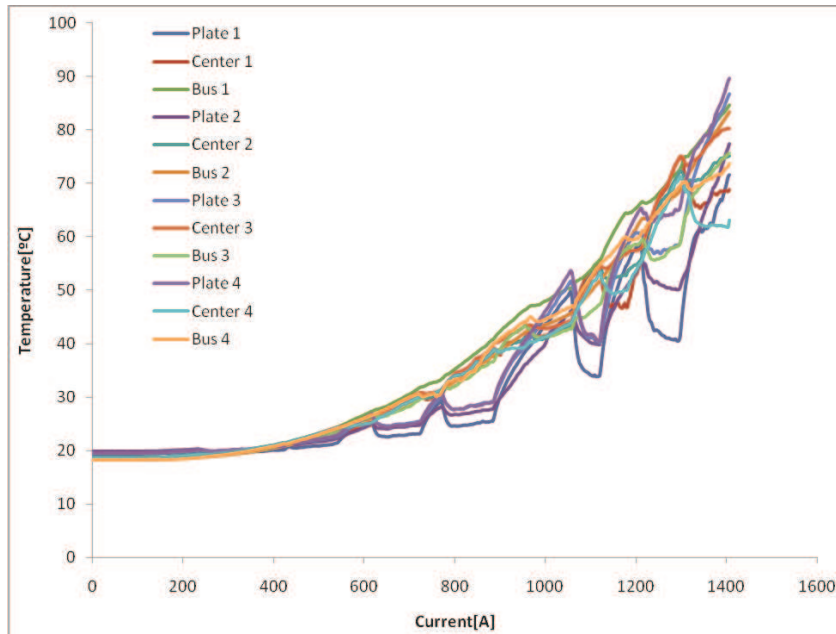


Fig. 37. Cable Test Result: Temperature vs. Current

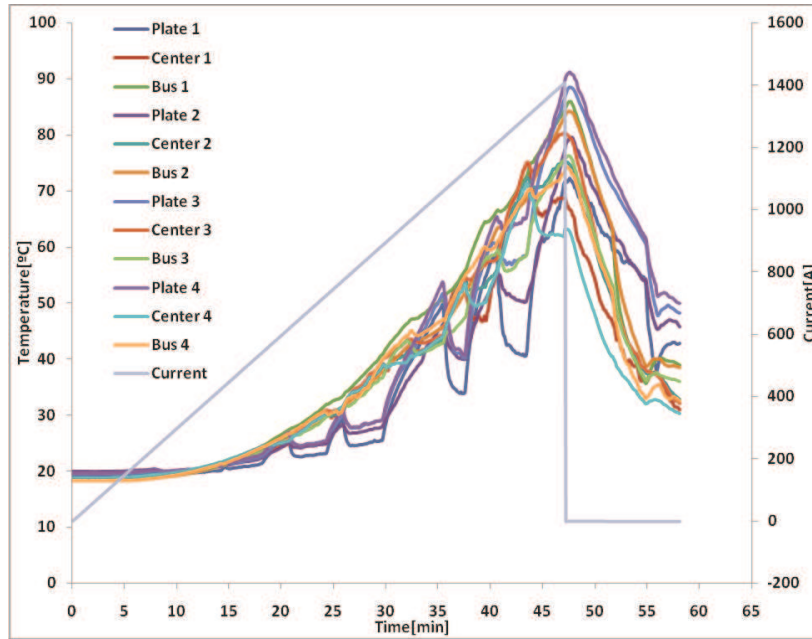


Fig. 38. Cable Test Result: Temperature vs. Time and Current

5.7. Test at 4.2 K

The model was warmed up after the 77K test and then placed into the dewer and cooled down with liquid helium. During the test at 4.2 K, the inserted voltage taps lost the contact to the YBCO tape, causing signal spike (shown in Figure 39). The signal spike exceeded the original test plan threshold. In order to overcome such issues the data acquisition system had to be modified. Table 9 lists the monitoring details for the coils and the corresponding protection.

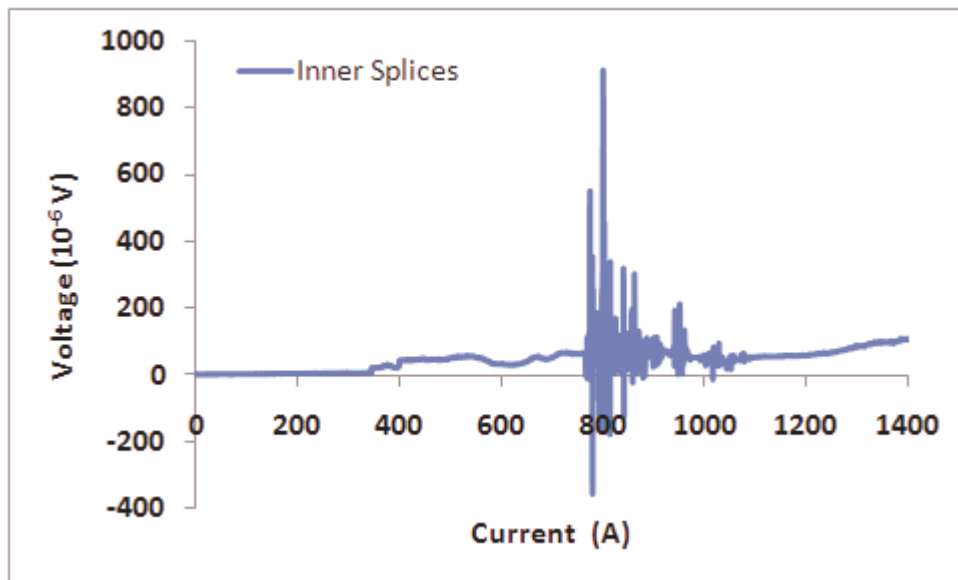


Fig.39. Signal Spike due to the Contact Voltage Taps

Table 9. Modified Data Acquisition Channels for Test at 4.2 K

Channel #	Section based on Voltage Tap	Description
1	VT8 to VT7	Coil 1: Outer splice
2	VT7 to VT9	Two Coils
3	VT4 to VT6	6 th turn of Coil 1 + inner splices + 6 th turn of Coil 2
4	--	Current lead (+) to Current lead (-)
5	VT6 to VT4	Reverse of CH3
6	VT9 to VT 10	Coil 2: Outer splice

The power supply was configured to shut down automatically at 1400 A. This limit was due to the safety issue of using four 15 feet long copper welding mentioned above. The voltage vs. current data acquired from CH1, CH2 and CH6 are shown in Figure 40. The resistance of the two outer splices is 17 nΩ and 141 nΩ, respectively. The resistance of the two coils including two inner splices is 174 nΩ.

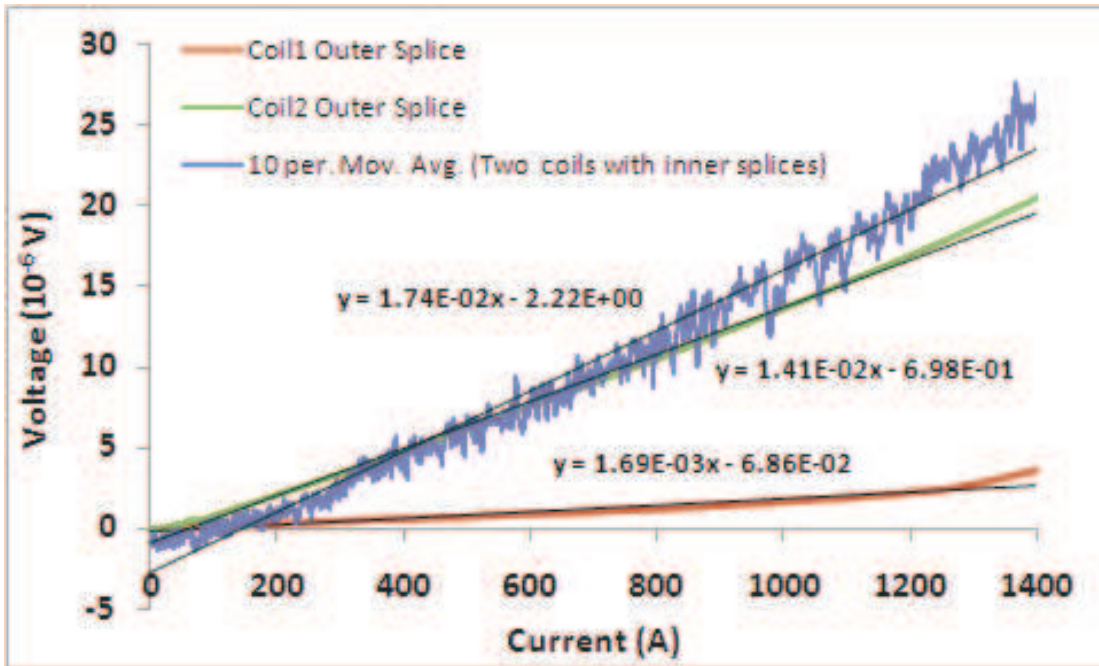


Fig.40. Data Acquisition and the Resistance of Each Channel

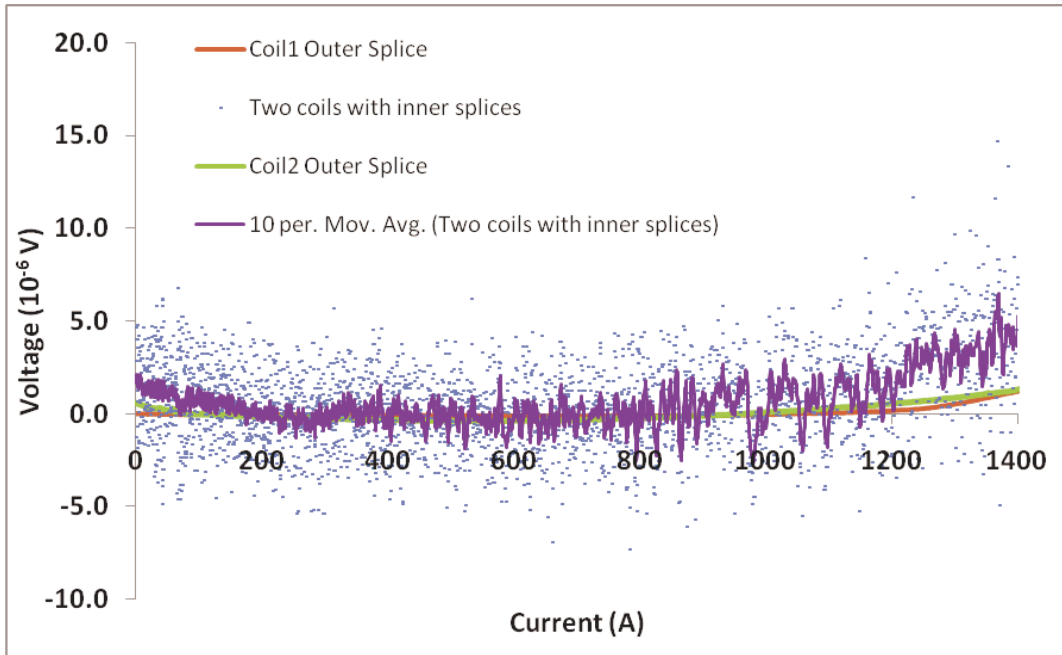


Fig.41. Processed Data on Each Channel

The data from each channel was trimmed by subtracting the amount $V = R \times I$ (R is the resistance, I is the corresponding current) to make the transition easier to observe. The processed data is shown in Figure 41. The test reached 1.4 kA, however the transition started in the coils at around 1.2 kA, about 82% SSL. The V-I curves bend at the beginning of the test, which indicates the superconductivity of the soldering material, Sn63%Pb37%, at low field/current. Figure 42 shows the performance comparison between the two magnets.

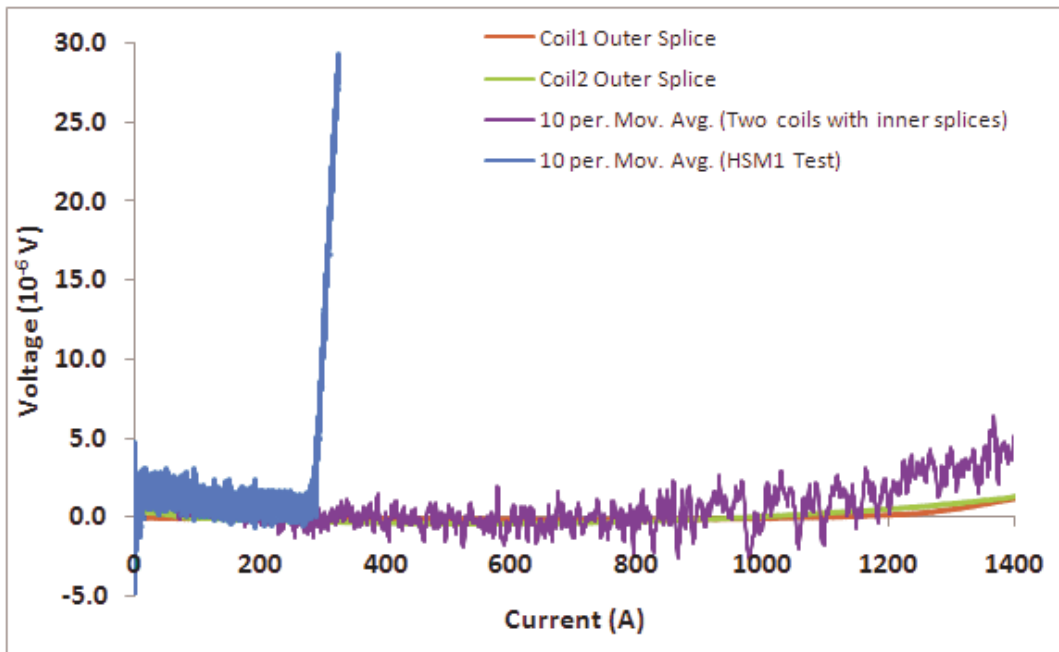


Fig. 42. The Performance Comparison between HSM1.1 and HSM1.

5.8. Test at 77 K Again

The model was warmed up to room temperature and then tested in liquid nitrogen. The performance of the magnet is shown in Figure 43. All the data were trimmed. The transition started at ~90 A in the inner splices section. The performance comparison with the first test at 77 K is shown in Figure 44. No degradation occurred during test at 4.2 K.

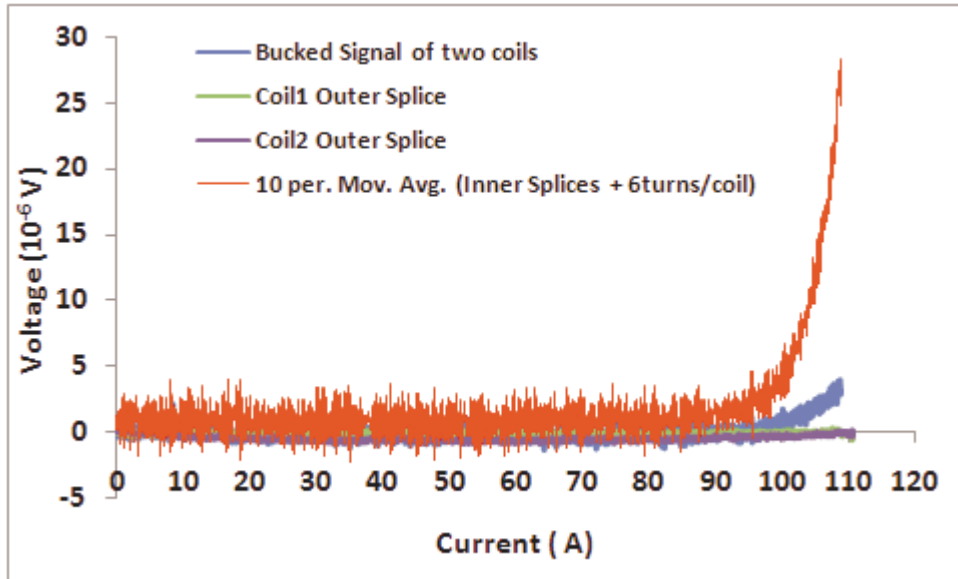


Fig. 43. Magnet Performance at 77 K after One Thermal Cycle.

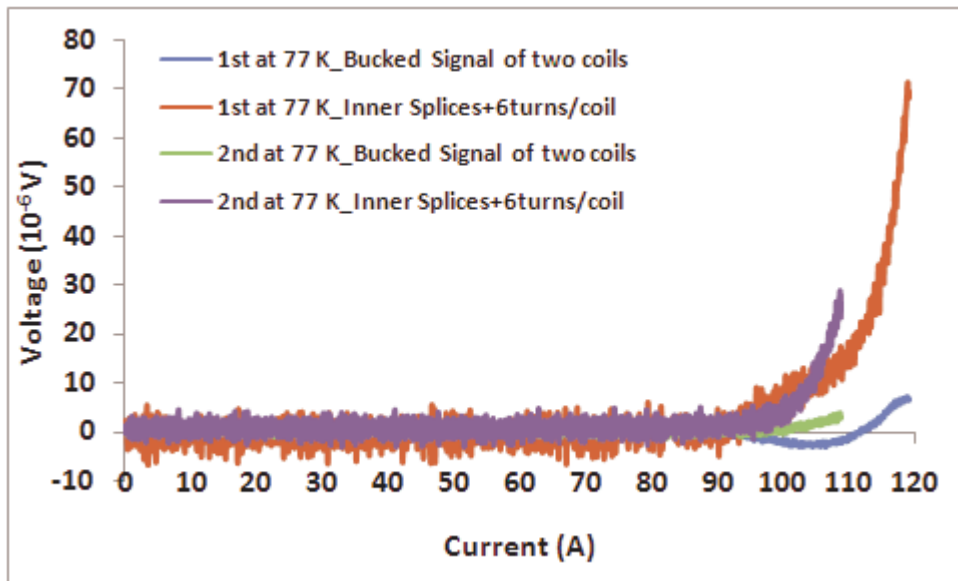


Fig. 44. Performance Comparison between Two Tests at 77 K

The comparison of the resistance measured at different temperature is listed in Table 10. The resistance of Coil 1 outer splice became much lower at 4.2 K than that at 77 K, from 60.6 nΩ to 17 nΩ. When the model was tested at 77 K again, the resistance of the

outer splice changed back to 60 n Ω . The other splices did not change too much during all the tests. The resistance of the splice needs more study and analysis.

Table 10. The Comparison of the Resistance Measured at 77 K and 4.2 K

	Resistance at 77 K (n Ω)	Resistance at 4.2 K (n Ω)	Resistance at 77 K (n Ω)
Coil1 Outer Splice	60.6	17	60
Coil2 Outer Splice	148	141	144
Inner Splices	174	174	155

6. Conclusion

The 1st helical solenoid double-pancake model was fabricated, and tested at both 77 K and 4.2 K successfully. The fabrication technology, including splicing and winding has been developed. The quench protection for testing at 4.2 K has been studied and developed. The model reached the reasonable performance.

The YBCO tape used in the 1st model was unwound and rewound several times, and no degradation was found in the tape.

7. Reference

- [1] Y. Derbenev and R. Johnson, "Six-dimensional muon cooling using a homogeneous absorber," *Phys. Rev. STAB*, 8, 041002, 2005.
- [2] K. Yonehara, Y. Derbenev, R. P. Johnson and T. J. Roberts, "Studies of a gas-filled helical muon cooling channel", *Proc. of EPAC2006*, Edinburgh, Scotland, 2006, pp. 2424-2426.
- [3] V.S. Kashikhin et al., "Four-coil superconducting helical solenoid model for Muon beam cooling," Proceedings of EPAC08, Genoa, Italy, 2008, pp. 2431-2433.
- [4] M. Yu et al., "Mechanical analysis and test results of 4-coil superconducting helical solenoid model," AIP Conference Proceedings, Volume 1218, pp. 515-522, 2009.
- [5] M. L. Lopes et al., "Studies of the high-field section for a muon helical cooling channel", *Proc. of PAC2009*, Vancouver, Canada, 2009, pp. 1-3.
- [6] D. Turrioni et al., "Study of HTS Wires at High Magnetic Fields", *IEEE Trans. on Applied Supercond.*, vol. 19, No. 3, June 2009.
- [7] E. Barzi et al, "BSCCO-2212 Wire and Cable Studies", presented at ASC 2010 and accepted for publication in *IEEE Trans. Appl. Sup.* (2011).
- [8] T. Shen et al., "Electromechanical Behavior of Bi-2212 Conductor Using a Split Melt Process for React-Wind-Sinter Magnet Fabrication", *IEEE Trans. on Applied Supercond.*, vol. 18, No. 2, June 2008.
- [9] A. Godeke et al., "Limits of NbTi and Nb₃Sn, and Development of W&R Bi-2212 High Field Accelerator Magnets", *IEEE Trans. on Applied Supercond.*, vol. 17, No. 2, June 2007.
- [10] Y. Xie et al., "Second-Generation HTS Wire for Magnet Applications," *21st Intern. Conference on Magnet Technology (MT-21)*, Hefei, China (2009).
- [11] K. Watanabe et al., "Thermal stability properties in Ag-sheathed Bi2212 superconductors with a very low resistive state", *Journal of the Cryogenic Society of Japan*, Volume 2, Number 7, 2007.
- [12] R.A. Badcock et al., "Progress in the Manufacture of Long Length YBCO Roebel Cables", *IEEE Trans. on Appl. Supercond.*, Vol. 19, Issue 3, 2009.
- [13] A. V. Zlobin et al., "Modeling the high-field section of a Muon helical cooling channel," Proceedings of IPAC'10, Kyoto, Japan, 2010, pp. 391-393.
- [14] S.A. Kahn et al., "Incorporating RF into a Muon helical cooling channel," Proceedings of IPAC'10, Kyoto, Japan, 2010, pp. 3509-3511.
- [15] V. Lombardo et al, "Critical current of YBCO Tapes and Bi-2212 Wires at Different Operating Temperatures and Magnetic Fields", presented at ASC 2010 and accepted for publication in *IEEE Trans. Appl. Sup.* (2011).